

# **New Perylene Diimide Dye Synthesis Containing Powerful Binding Sites For Metal Ions**

**Courage Iboro Akpan**

Submitted to the  
Institute of Graduate Studies and Research  
in partial fulfilment of the requirements for the degree of

Master of Science  
in  
Chemistry

Eastern Mediterranean University  
July 2016  
Gazimağusa, North Cyprus

Approval of the Institute of Graduate Studies and Research

---

Prof. Dr. Cem Tanova  
Acting Director

I certify that this thesis satisfies the requirements as a thesis for the degree of Master of Science in Chemistry.

---

Prof. Dr. Mustafa Halilsoy  
Chair, Department of Chemistry

We certify that we have read this thesis and that in our opinion it is fully adequate in scope and quality as a thesis for the degree of Master of Science in Chemistry.

---

Prof. Dr. Huriye İcil  
Supervisor

---

Examining Committee

1. Prof. Dr. Huriye İcil

---

2. Asst. Prof. Dr. Süleyman Aşır

---

3. Asst. Prof. Dr. Nur P. Aydınlık

---

## ABSTRACT

Metal binding is expected to make changes in photophysical and photochemical properties of sensitizers such as wavelength shifts and intensity changes in absorption and emission spectra. Perylene chromophoric dyes are excellent materials of aromatic  $\pi$ -conjugated heterocyclic family. The rigid structure of perylene chromophores causes strong intermolecular  $\pi$ - $\pi$  interactions giving rise to versatile optical and electronic characteristics. With the advantages of tailoring the imide and bay-positions of perylene structures, exclusive benefits were achieved such as n-type semiconducting character, extended absorption coefficients, high photoluminescence quantum yields, self-assembly behaviours, thermal and photostabilities.

A new perylene diimide dye containing powerful binding site for metal ions was synthesized successfully. The synthesized product was characterized by FTIR, UV-vis, emission, TGA, DSC and elemental analysis. In addition, the photophysical properties were investigated in detail. The high thermal and photostabilities, including important photonic properties, make the new dye a potential candidate for various photo-sensing applications.

**Keywords:** perylene dyes, hydrogen bond donor, metal binding

# ÖZ

## ACKNOWLEDGMENT

I gratefully express All Praise to God Almighty for His continuous faithfulness and love.

I would like to express my heartfelt gratitude to my supervisor, **Prof. Dr. Huriye İcil** for the opportunity given to me to work in her research group. Her valuable contributions and enriching suggestions are matchless. I admit that she was a source of inspiration and motivation all through this research period.

Special thanks to Dr. Duygu, and Basma for their guidance and help in the laboratory.

I would also like to appreciate all other members of the İcil's Organic Research Group, including Melika, Meltem, Selin, Sümeyye, Adamu, Hengameh for their friendship.

Thanks to my special friends; Victor, Michael, Femi, Chijioke, Kayode, Dammy, Kayode, Ailem, Nancy espoir, Pastor Alola, Pastor Abiola's families, Word miners, all leaders and workers of Shekinah parish.

My deepest gratitude goes to my beloved parents: Mr Francis and Mrs Victoria Akpan for their priceless love, encouragement, and sacrifice and prayers. Thanks to my siblings, Mary, Emmanuel, Israel, God'swill. My cousins; Patience and Sunday. God bless you all. Amen.

# TABLE OF CONTENTS

ABSTRACT.....	iii
ÖZ.....	iv
ACKNOWLEDGMENT.....	v
LIST OF TABLES.....	viii
LIST OF FIGURES.....	ix
LIST OF ILLUSTRATIONS.....	xi
LIST OF ABBREVIATIONS.....	xii
1 INTRODUCTION.....	1
1.1 Perylene Dyes.....	1
1.2 Hydrogen Donor Perylene Diimide.....	3
1.3 Interaction of Metal With Ligands.....	5
2 THEORETICAL.....	8
2.1 Synthesis and Applications of Perylene Dyes.....	8
2.2 Energy Transfer.....	10
2.3 Electron Transfer.....	13
2.4 Organic Solar Cells and their Applications.....	14
3 EXPERIMENTAL.....	17
3.1 Materials.....	17
3.2 Instruments.....	17
3.3 Method of Synthesis.....	18
3.4 Synthesis of T-PDI.....	19
3.5 General Synthetic Mechanism of Perylene Dyes.....	21
4 DATA AND CALCULATION.....	25

4.1 Optical and Photochemical Properties .....	25
4.1.1 Molar Absorption Coefficient ( $\epsilon_{\max}$ ).....	25
4.1.2 Florescence Quantum Yield ( $\phi_f$ ).....	26
4.1.3 Half Width of the Selected Absorption Band ( $\Delta\bar{\nu}_{1/2}$ ) .....	28
4.1.4 Theoretical Radiative Lifetime ( $\tau_0$ ).....	30
4.1.5 Theoretical Fluorescence Life Time ( $\tau_f$ ) .....	31
4.1.6 Fluorescence Rate Constants ( $k_f$ ) .....	32
4.1.7 Rate Constants of Radiationless Deactivation ( $k_d$ ).....	33
4.1.8 Oscillator Strength ( $f$ ).....	34
4.1.9 Singlet energies ( $E_s$ ).....	35
5 RESULTS AND DISCUSSION .....	56
5.1 Synthesis and Characterization .....	56
5.1.1 Analysis of IR Spectra .....	57
5.2. Absorption and Fluorescence Properties.....	58
5.2.1 Analysis of UV-vis Absorption Spectra of T-PDI .....	58
5.2.2 Analysis of Emission Spectra of T-PDI.....	59
5.3 Thermal Stability.....	59
6 CONCLUSION .....	61
REFERENCES.....	63
APPENDIX.....	70
Appendix A: Curriculum Vitae.....	71

## LIST OF TABLES

Table 4.1: Molar absorptivity data of T-PDI in TFA, DMF and NMP.....	25
Table 4.2: Half width of PDI in different solvents.....	29
Table 4.3: Theoretical radiative lifetime of T-PDI in different solvents .....	30
Table 4.4: Theoretical fluorescence life time ( $\tau_f$ ) in different solvents.....	31
Table 4.5: Fluorescence rate constants of PDI in different solvents.....	32
Table 4.6: Rate constants of radiationless deactivation ( $k_d$ ) in DMF and NMP .....	33
Table 4.7: The oscillator strength of PDI in other solvents .....	34
Table 4.8: Single energies of PDI in different solvents are summarized below .....	35
Table 5.1: Solubility of the synthesized perylene derivative (T-PDI) .....	55



## LIST OF FIGURES

Figure 1.1: The General Structure of Perylene Diimide .....	1
Figure 1.2: Scheme of Hydrogen Bond Donor and Acceptor .....	3
Figure 1.3: Amines; 4,6-diamino-2-pyrimidinethiol (1.2a) and melamine (1.2b) with H-bond donor sites .....	4
Figure 1.4: Structure of Perylene Diimide .....	6
Figure 1.5a: 3D Structural Representation of T-PDI ..	6
Figure 1.5b: 3D Structural Representation of T-PDI ..	6
Figure 2.1: Symmetrical (right) and Asymmetrical (left) Perylene Diimides with peri, ortho and bay positions .....	8
Figure 2.2: Coulombic Exchange Mechanism .....	12
Figure 2.3:D-A Photoinduced Charge Transfer. (a) ET (D* - PDI) (b) ET (D – PDI*).....	14
Figure 2.4: Model of Solar Cell and Panel.....	15
Figure 3.1: Structure of T-PDI.....	19
Figure 4.1: Jablonski Diagram .....	25
Figure 4.2: Representative Half-Width Plot on the Absorption Spectrum of T-PDI in TFA .....	27
Figure 4.3: FTIR spectrum of 4,6-Diamino-2-pyrimidinethiol.....	35
Figure 4.4: FTIR spectrum of PDA.....	36
Figure 4.5: FTIR spectrum of T-PDI .....	37
Figure 4.6: Absorbance spectrum of 4,6-Diamino-2-pyrimidin-thiol in DMF.....	38
Figure 4.7: Absorbance spectrum of PDA in DMF .....	39
Figure 4.8: Absorbance spectrum of T-PDI in DMF .....	40

Figure 4.9: Absorbance spectrum of T-PDI in DMF after microfiltration (0.2 $\mu$ m)...	41
Figure 4.10: Absorbance spectrum of T-PDI in NMP .....	42
Figure 4.11: Absorbance spectrum of T-PDI in NMP after microfiltration (0.2 $\mu$ m).	43
Figure 4.12: Absorbance spectrum of T-PDI in TFA .....	44
Figure 4.13: Absorbance spectrum of T-PDI in DMF, NMP and TFA .....	45
Figure 4.14: Emission spectrum ( $\lambda_{exc} = 485nm$ ) of T-PDI in DMF .....	46
Figure 4.15: Emission spectrum ( $\lambda_{exc} = 485nm$ ) of T-PDI in DMF after microfiltration (0.2 $\mu$ m).....	47
Figure 4.16: Emission spectrum ( $\lambda_{exc} = 485nm$ ) of T-PDI in NMP .....	48
Figure 4.17: Emission spectrum ( $\lambda_{exc} = 485nm$ ) of T-PDI in NMP after microfiltration (0.2 $\mu$ m).....	49
Figure 4.18: Emission spectrum ( $\lambda_{exc} = 485nm$ ) of T-PDI in TFA .....	50
Figure 4.19: Emission spectrum ( $\lambda_{exc} = 485nm$ ) of T-PDI in DMF, NMP and TFA .....	51
Figure 4.20: DSC Curve of T-PDI at a heating rate of 10 <sup>0</sup> C / min in nitrogen.....	52
Figure 4.21: TGA Thermogram of T-PDI at heating rate of 10 <sup>0</sup> C / min in oxygen .	53

## LIST OF ILLUSTRATIONS

Scheme 3.1: Synthesis of T-PDI.....	18
Scheme 3.2: General Synthetic Mechanism of Perylene Dyes .....	21

## LIST OF ABBREVIATIONS

Å	Armstrong
AU	Arbitrary Unit
Cm	Centimetre
CCl <sub>4</sub>	Carbon tetrachloride
°C	Degree celcius
CHCl <sub>3</sub>	Chloroform
DMF	N,N'-dimethylformamide
DSC	Differential Scanning Calorimetry
DSSC	Dye-sensitized Solar Cell
DCM	Dichloromethane
D-A	Donor -Acceptor
$\epsilon_{\max}$	Maximum extinction coefficient
E <sub>s</sub>	Singlet energy
FTIR	Fourier Transform Infrared Spectroscopy
F	Oscillator strength
H	Hydrogen
kcal	Kilocalorie
k <sub>f</sub>	Fluorescence rate constant
k <sub>d</sub>	Rate constant of radiationless deactivation
M	Molar concentration
min	Minute
mmol	Millimole
NMP	N-Methyl-2-pyrrolidone

nm	Nanometer
OFET	Organic field-effect transistor
OLED	Organic Light Emitting Diode
OPV	Organic Photovoltaics
PDI	Perylene diimide
PDA	Perylene-3,4,9,10- tetracarboxylic dianhydride
PET	Photoinduced Electron Transfer
TGA	Thermogravimetric analysis
TCE	Trichloroethylene
TFA	Trifluoroacetic acid
T-PDI	Thiol-perylene diimide
$\tau_0$	Theoretical Radiative lifetime
$\tau_f$	Fluorescence lifetime
$\mu$	Micro
UV-vis	Ultraviolet visible
$\Delta v_{1/2}$	Half-width of the selected absorption
$\nu$	Wavenumber
$\lambda_{exc}$	Excitation wavelength
$\lambda_{max}$	Absorption wavelength at maximum

# Chapter 1

## INTRODUCTION

### 1.1 Perylene Dyes

Perylene dyes were originally industrial dyes and pigments; however more recently they are referred to as ‘functional dyes’ because of their high optical properties.

Perylene dyes are perylene – 3,4,9,10 – tetracarboxylic acid diimide derivatives, and also referred to as perylene diimides (PDIs). Perylene dyes have been utilized as colorants in supramolecular dye chemistry for their pigments and industrial applications [1]. In 1913, Kardos investigated and reported the chemistry of perylene and its derivatives [2-3] and since then, they have been extensively used in various applications such as photonics, photovoltaic cells and lasers, Organic Light Emitting Diodes (OLEDs) and Organic Field-Effect Transistors (OFETs).

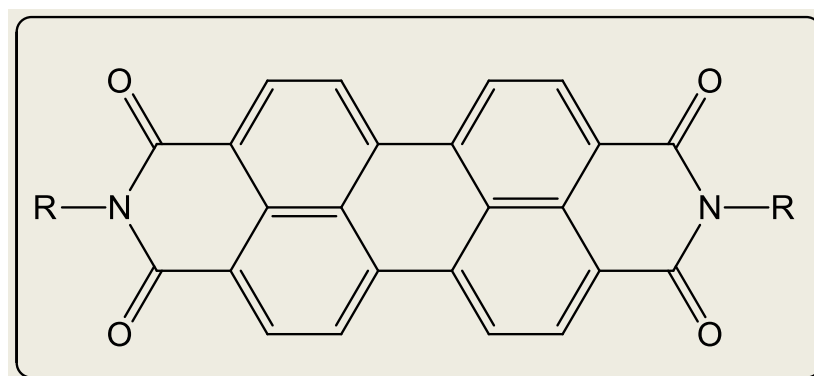


Figure 1.1: The General Structure of Perylene Diimide

Perylene – 3,4,9,10 – tetracarboxylic dianhydride (PTCDA) is the parent compound for preparing PDI materials, usually by condensation reaction with an alkyl amine [4]. Perylene dyes have been of tremendous interest among researchers as a result of their structural and functional properties. Structurally, as shown in Fig 1.1, perylene dye contain a pi-conjugated rigid blocks with phenyl groups attached, hence its strong intermolecular pi-pi interaction giving rise to versatile optical and electronic characteristics. Furthermore, its rigid and aromatic pi-conjugated core structure best explains the reason for insolubility and migrational stability in organic solvents. However, a level of solubility of PDI in organic solvents is expected for continuous and feasible applications in electronic and photovoltaics field.

PDI's are known for their high fluorescence quantum yield, high chemical, thermal and photochemical stabilities [5]. These excellent photophysical properties make PDI derivatives excellent material in various applications in organic semiconducting systems [6], solar cells [7], organic field effect transistors (OFETs) [8] and in photovoltaics devices [9].

Also, in past years, huge research has so far witnessed in donor-acceptor based systems owing to the functional properties of PDI's stated above [10].

With the possibility of tailoring the imide and bay positions of PDI structures, researchers continuously derive novel exclusive benefits in n-type semiconductors, extended absorption coefficients, high fluorescence quantum yield, self-assembly patterns, thermal and photostabilities [11]. This functionalization provides extra force such as static interaction, dipole moment, hydrophobic/hydrophilic interaction etc.

Several other structures such as nanotubes [12], nanofibers [13] and nanoparticles [14] are developed after successful functionalization.

The imide and bay substitution sites of PDI are point of attachment for substituents of chromophores. The bay substitution is primarily utilized for optical and electrochemical properties while the imide substitution affects aggregation and solubility.

## 1.2 Hydrogen Donor Perylene Diimide

Hydrogen bond donor is the hydrogen attached together with an electronegative (–) molecule eg. fluorine (F), oxygen (O) and nitrogen (N) (Figure 1.2).

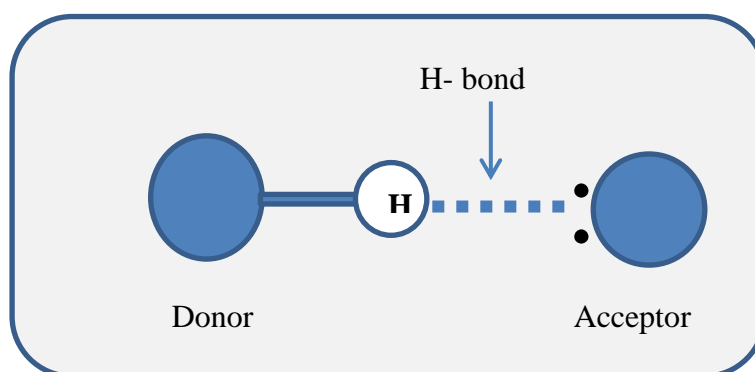


Figure 1.2: Scheme of Hydrogen Bond Donor and Acceptor

Researchers have developed keen interest in the complexation of organic dyes which give rise to the formation of supramolecular assemblies. The assemblies are held together by noncovalent bonding like H-bonding, pi-pi stacking and metal ion coordination [15]. This approach to an ordered perylene diimide assembly have led to more detailed studies of pi-pi interactions and hydrogen bonding [16].



Hydrogen bonding is known for its directionality and specificity, hence its usefulness in supramolecular systems. Due to these properties, Young and co-workers synthesized PDI derivative with hydrogen bonding moieties with the future aim of developing functional devices [17].

Also, Würthner et. al. reports the application of hydrogen bonding of PDIs with ditopic melanines including well defined geometries [18]. Their argument for the imide-melanin association was based on the three hydrogen bonds that provide strong directionality.

Melamine and 4,6-diamino-2-pyrimidinethiol can be utilized for imide substitution on perylene derivative. Fig 1.3 shows the two amine, having  $-NH$  Hydrogens (H-bond donors), with exception to  $-SH$  group because of its lower electronegativity and bond energy of 2.58 and 1.0 kcal/mol, respectively.

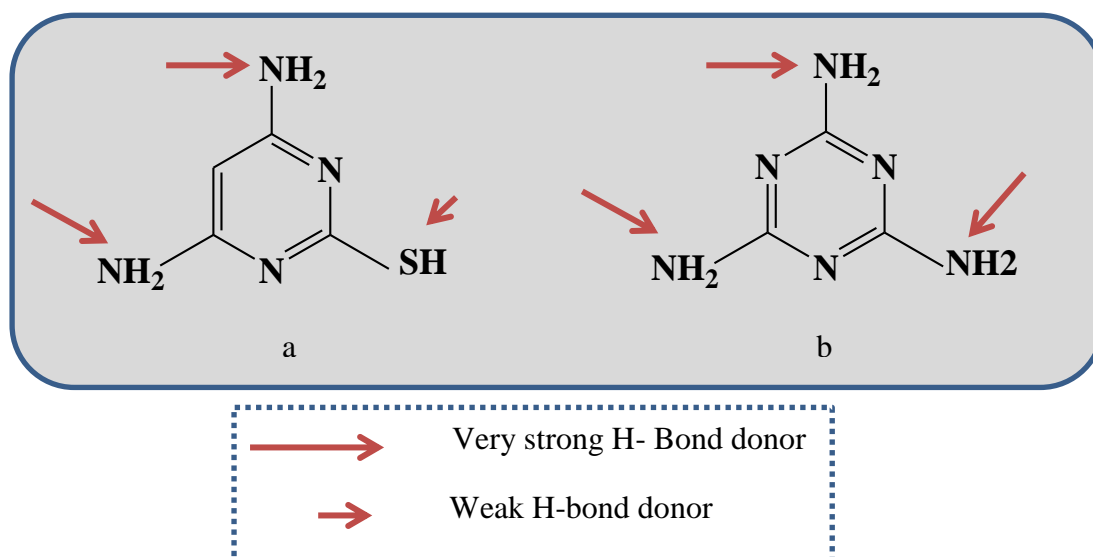


Figure 1.3: Amines; 4,6-diamino-2-pyrimidinethiol (a) and melamine (b) with H-bond donor sites.

### 1.3 Interaction of Metal With Ligands

Generally, ligands are molecules, atoms or ions covalently bounded in a coordination complex with a metal. Ligands, also called Lewis bases, act as electron pair donors while the central metal atom, referred to as Lewis acids, act as electron pair acceptors. This interaction by covalent bonds therefore leads to a coordination complex. The complex type or geometry is a function of the number of ligand on the central atom. The geometries for two, three, four ligands are linear, tetrahedral or square planar and octahedral, respectively.

Metal complexes were first prepared by Fujita et al [19]. Würthner later adopted his concept of macrocyclic metal complexes to prepare a square-like perylene diimide ligands, complex with platinum (Pt) metal [20-21].

Organic dyes optical properties are at the premise of many novel structures like OFETs and OLEDs structures [22-23]. Thus, perylene diimide derivatives are regarded as excellent candidates for organic electronic devices due to its potentials. Their chromophores have orbital nodes in Highest Occupied Molecular Orbital (HOMO) and Lowest Unoccupied Molecular Orbital (LUMO) at the peri nitrogen's, resulting to a decoupling of the chromophore owing to the single bonds [24].

PDI derivatives are also excellent materials for metal ion receptor. Monovalent metal ions such as Ag, Au and Cu are well reported in the literature for their excellent emissive properties [25], hence understanding metal and organic interface is tantamount to high quality OFET structures [26]. Metals such as iron, copper, zinc etc. binds to PDIs sites, influencing significant changes in the photophysical and photochemical properties of sensitizers as wavelength shift, absorption and emission

spectra. At the same time, the binding groups improve the solubility of PDIs by reducing the pi-pi stacking and hence ensuring good electron accepting capability [27-28].

In the light of these, this thesis therefore aimed to synthesis of a novel PDI that has sites for metallic ion bonding. The synthesized product is characterized by FTIR, NMR, UV-Visible, emission, Differential Scanning Calorimetry, Thermogravimetric analysis and elemental analysis. Also, photophysical properties investigated in detail.

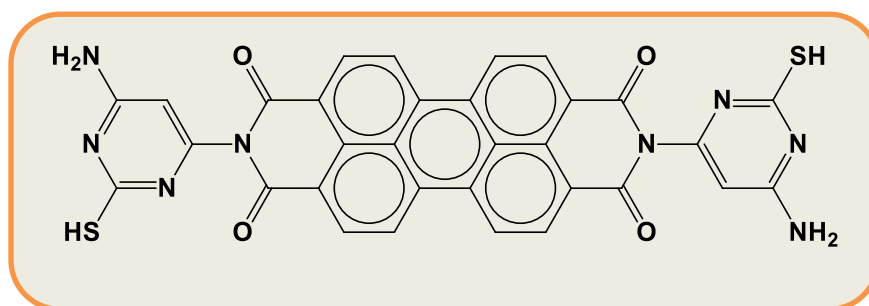


Figure 1.4: Structure of T-PDI

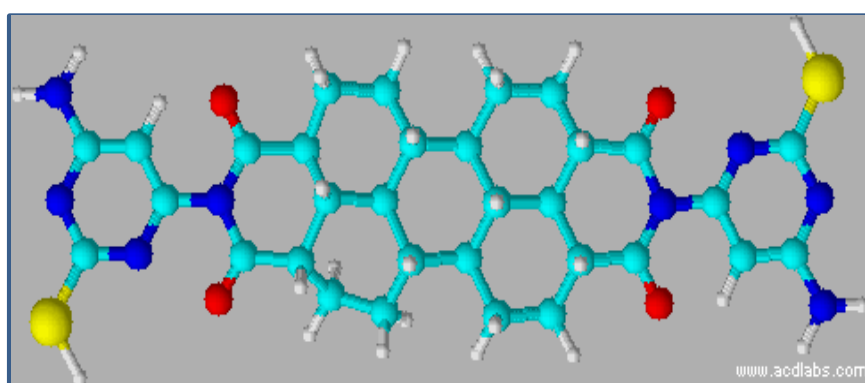


Figure 1.5a: 3D Structural Representation of T-PDI

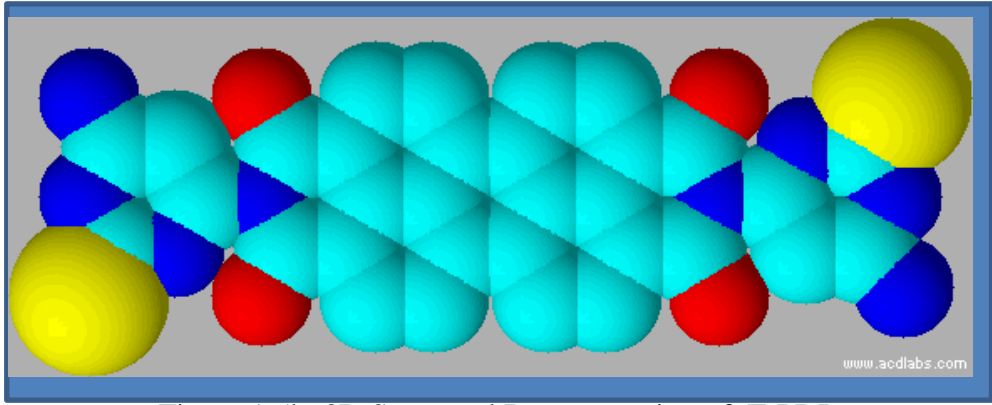


Figure 1.5b: 3D Structural Representation of T-PDI

## Chapter 2

### THEORETICAL

#### 2.1 Synthesis and Applications of Perylene Dyes

Generally, the synthesis of perylene dyes undergoes condensation reaction of the starting material, perylene-3,4,9,10-tetracarboxylic dianhydride and an amine usually in the presence of a solvent and a catalyst [29-30]. The reactivity of the amine is a function of the choice of solvent used. For less reactive amines such as the aromatic amines, solvents like quinolone etc. are essentially used at 160-180°C. Water, DMF, and other alkyl amines are used for reactive amines at temperature below 160°C. Zinc acetate, suggested to increase the solubility of the anhydride is used as catalyst in the synthesis of perylene dyes.

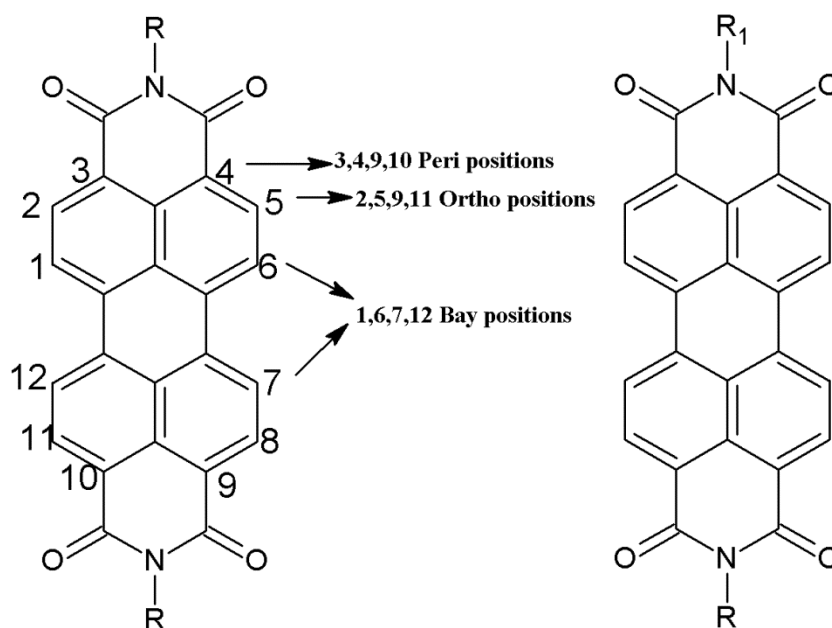


Figure 2.1: Symmetrical (Right) and Asymmetrical (Left) Perylene Diimides with Peri, Ortho and Bay Positions.

Non-symmetrically substituted perylene derivatives are formed by multistep process [31-32]. The symmetrically substituted perylene dyes undergoes saponification by potassium salt (potassium hydroxide). A monoimide anhydride is formed after reaction with acid, react with an amine. The product formed is a non-symmetrical substituted perylene diimides.

Two major approaches for substitution exist in perylene dimide structure; the imide and the bay substitution. The former affects solubility and the bay substitution affects functionality. Langhals et. al. reports the presence of alkyl substituents with long chain at the imide position which subsequently increase solubility [33]. By this substitution, the nodes of the HOMO and LUMO at the imide position decreases the coupling (non-conjugation) of PDI core and imide substituents.

By the emergence of decoupling, the absorption and emission features of Perylene diimide remains unchanged but gives a high fluorescence yield with a small stoke shift in spectra – (absorption and emission spectra). This is because the perylene core is not affected by imide substitution. Another approach of substitution is the bay substitution on the 1,6,7 and 12 position of the perylene core described by Seybold and coworkers. Many tetra- and di-substituted materials have been synthesized because of the ease of control of these substituents (carbon, cyano, oxygen, nitrogen, bromine, chlorides) at the 1,6,7 and 12 positions. Jiajus Ma et. al. synthesize 1,7-dibromo substituted PDI (60%) [34] and Tyler Clikeman et. al. also designs via bay and ortho polyTFM PDI [35]. Bay substitution broadens the absorption and emission spectra, increases stoke shift and decreases fluorescence quantum yield.

The derivatives of PDIs were originally used as industrial dyes but presently been

used in several applications due to the excellent properties of PDIs, ranging from optical to thermal properties and from photochemical to electrochemical properties. All the above properties arise from the strong pi-pi interaction of the aromatic core. Perylene derivatives are useful materials in organic solar cells, dye lasers, photovoltaic cells, OFETs, LEDs, light harvesting arrays, wires, Liquid Crystal Displays (LCD) filters etc.

The leading lights of these possible PDI applications is the ease of improving the dyes, and its electron acceptor capabilities while controlling features such as solubility and stability.

Solar cells devices converts solar energy to electricity. The success of this application is attributed to the planar nature, high electron affinity and mobility of PDI in the literature. Low solubility's in solution accounts for PDIs use as fluorescent labels or tags. They also thrive in OFETs and organic photovoltaics (OPVs) due to strong electron transports in PDIs. Light emitting ability is a property of PDI which favours it utilization in laser dyes and OLEDs.

Another application area is in photonics. Here, photons are used to generate, process and transmit information. Scientists have explored areas of optical processing and storage of information which is of great interest in technology (Burzynski R, et. al. 1994).

## **2.2 Energy Transfer**

The emission of a donor molecule and the subsequent absorption by an acceptor molecule is known as Energy Transfer or Resonant Energy Transfer. Upon

excitation, the donor molecule (D) absorbs and transfers excitation energy to an acceptor molecule A which becomes excited, A\*. The donor emission undergoes quenching and the other charge transfer.

Two classes of energy transfers have been studied; the radiation or trivial and Non-radiative or radiationless energy transfer.

During the radiative energy transfer, photons are emitted. A donor chromophore, D is excited and raised to an excited state D\*. The excited molecule decays and emits energy that is absorbed by an acceptor molecule, A which results in A\*.



Contrarily, the excited donor interacts with the acceptor molecule, A during the radiationless energy transfer. Both categories require an overlapping of donor and acceptor molecules as criteria. In a photophysical process, studies have shown that the excitation energy usually from a D-A occurs at a distance (Armstrong) of 1.5-10 nm [36-37]. Förster describes this occurrence as a result of long dipole-dipole interaction between both molecules where the photon is eventually lost [38]. In another study conducted by Dexter, energy transfer occurs by orbital overlap which limits distances between chromophoric units. Overlapping between the D-A spectrum results in the production of resonant transitions.

The Förster type mechanism also called Coulombic mechanism requires no contact between acceptor and donor molecules, since transitions possess high oscillator strength. A good example is the singlet-singlet (S-S) energy transfer. On the other



hand, Dexter type mechanism also called Exchange mechanism is known to be short ranged and occurs by orbital overlap.

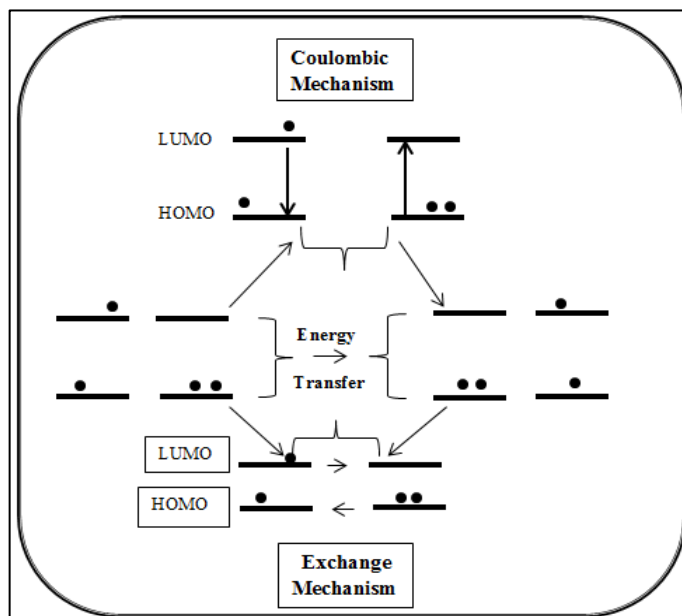


Figure 2.2: Coulombic and Exchange Mechanisms

This mechanism requires that spin conservation be obeyed especially in cases where the excited states involves spin forbidden transition. A typical example is the triplet-triplet energy transfer (Straight 2002, Prevost 2001). However, the efficiency of energy transfer is denoted as

$$\Phi_T = \frac{1 - \Phi_D}{\Phi_D^0} \quad \text{Equ (2.2.4)}$$

$\Phi_T$  = Efficiency of energy transfer

$\Phi_D$  = Quantum yield of donor (in the presence of acceptor)

$\Phi_D^0$  = Quantum yield of donor (in the absence of acceptor)

## 2.3 Electron Transfer

During chemical reactions, an electron is transferred from one molecule to another molecule, reducing the former while the latter is oxidized. In other word, two important conditions must be satisfied for transfer of electrons in a D-A system. Firstly, the reaction must release energy (exergonic reaction) and secondly, sufficient rate of reaction is accounted for (kinetic reaction).

With respect to D-A type systems such as perylene diimides in literatures, the kinetic and thermodynamics have been elucidated by Rehn Weller equation [39] and Marcus Theory [40-41]. R.Weller describes the driving force ( $\Delta G_{CS}$ ) of charge transfer including changes in Gibbs free energy. Optical molecules are activated by photons and undergo reductive-oxidative reaction, thereby converting solar to chemical energies through charge separation [42]

$$\Delta G_{CS} = e[E^{1/2}(D/D^{+\bullet}) - E^{1/2}(A^{-\bullet}/A)] - E_{(0,0)} - E_{coul} \quad \text{Equ (2.3.1)}$$

$E^{1/2}(D/D^{+\bullet})$  : Electrochemical half wave potential in relation to oxidation in D

$E^{1/2}(A^{-\bullet}/A)$  : Electrochemical half wave potential in relation to reduction in A

$E_{(0,0)}$  : Energy of singlet state

$E_{coul}$  : Coulombic stabilization energy

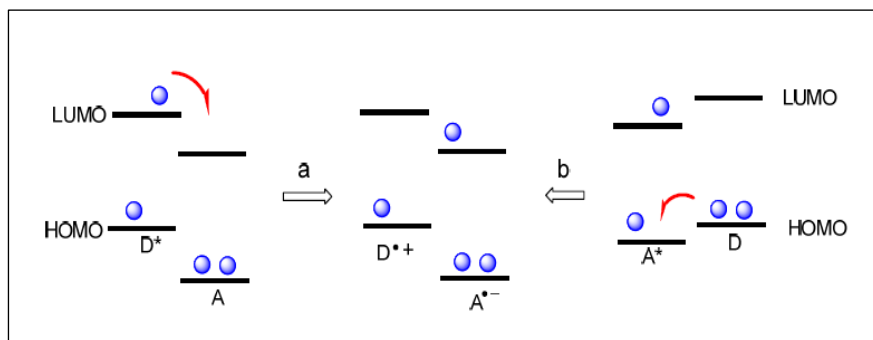


Figure 2.3: D-A Photoinduced charge transfer. (a) ET (D\* - PDI) (b) ET (D – PDI\*)

Marcus describes the rate of electron transfer (ET). The important features of Marcus theory are free energy ( $\Delta G_{CS}$ ) and reorganization energy ( $\lambda$ ). In determining the rate of ET, distance and orientation are important factors to consider.

$$\Delta G^\ddagger = \frac{\Delta G_{CS} + \lambda}{4\lambda} \quad \text{Equ ( 2.3.2)}$$

Perylene derivatives can electrochemically transfer or accept electron but primarily act as electron acceptors and are used in diverse excited - state electron transfer processes.

## 2.4 Organic Solar Cells and their Applications

A solar cell or photovoltaic (PV) cell is simply an electronic device that converts sunlight to electrical energy. A calculated value of about  $1.34 \times 10^{31}$  J of energy radiates the earth per day, a free and plentiful source which scientist have explored for solar cell technologies.

The first working solar or photovoltaic cell was constructed by C Fritts, with a melted non-metal with semiconducting features (selenium) on a metal surface [43].

The motivation of researchers to generate power led to the development of modern time solar cells to supply energy. Solar cells are durable with a less maintenance/ light installations and its non-polluting.

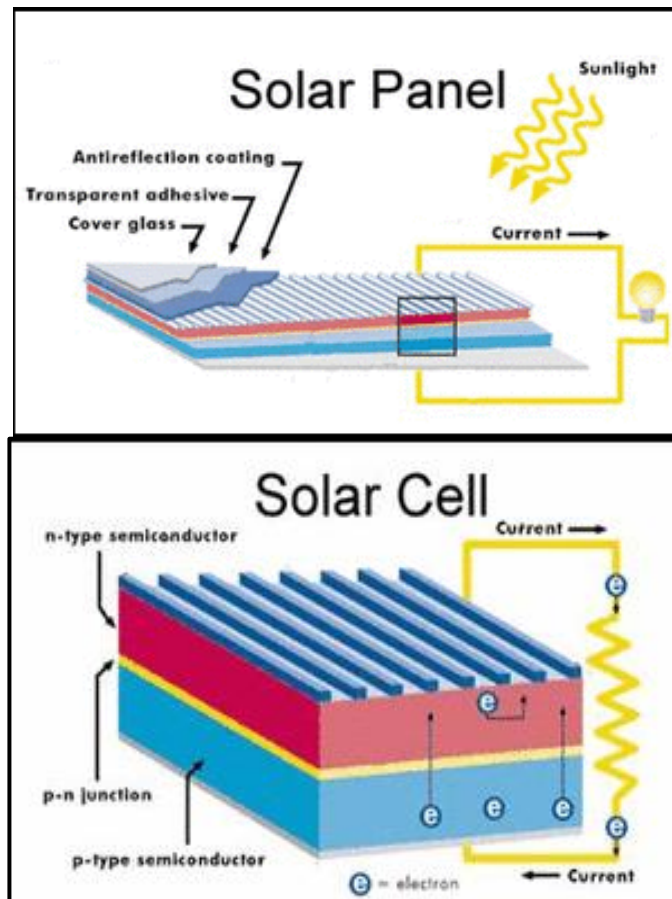


Figure 2.4: Model of Solar cell and panel. (TAN Ying-Xiong, et al, 2014)

Solar cells consist of materials known as semiconductors, which are characteristic of absorbing light eg. silicon. Depending on the number of layers of the absorbing material, solar cells are either single-junctioned or multi-junctioned necessary for charge separation [44]. When light hit the cell, an electron hole is created. The semiconducting material releases electron to flow freely in a direction. The electric field present in the cell forces electron to the external circuit. The electron can move in the direction of n and p side based on proximity of the free electron and electric field. The solar cell's electric field and electron flow give rise to the voltage and current, respectively. Having the voltage and current produces power. This led to the estimation of the efficiency of a homojunction solar cell by William and Hans [45].

Solar cell technology can be described according to material made up of. The first generation solar cells are the single crystal (Si), a wafer or silicon-material solar cell. The development of thin film industries led to the second generation PV cells, (thin film solar cell) that consist of amorphous silicon important in building PV stations. The third generation solar cells is currently an ongoing research work which include the dye sensitized solar cells.

However, demands made on affordable PV cells has brought about the development of polymer PV cells because of its cheaper cost compared to silicon based semiconductors. PDI based materials have immensely contributed, by utilization, as organic semiconducting material in solar cells. They have received much focus because of their pi-conjugated structure and photoelectric features with excellent prospect [46]. Therefore, applications in the field of charge separation, synthesis and characterization of perylene derivatives, OLED and photovoltaic cells have thrived recently [47].

## Chapter 3

### EXPERIMENTAL

#### 3.1 Materials

Perylene-3,4,9,10-tetracarboxylic dianhydride (PDA), 4,6-diaminopyrimidine-2-thiol, isoquinoline, *m*-cresol, methanol and zinc acetate were all obtained from Sigma Aldrich. Methanol, acetone and chloroform were purified by distillation while the other chemicals were used without further purification. Liquid reagents were dried by Molecular sieves (4-8 mesh).

Pure spectroscopic grade solvents were used for all spectroscopic analysis. All reactions were monitored by Thin Layer Chromatography (TLC, aluminium sheets of  $5 \times 10$  cm silica gel 60 F<sub>254</sub>) and visualized by UV light.

#### 3.2 Instruments

Infrared Spectra (IR) were recorded with KBr pellets using JASCO FTIR 6200.

Ultraviolet Absorption Spectra (UV-vis) were recorded with Cary-100 UV visible spectrophotometer.

Emission Spectra and Florescence Quantum Yield were calculated by Varian Cary Eclipse Fluorescence Spectrophotometer.

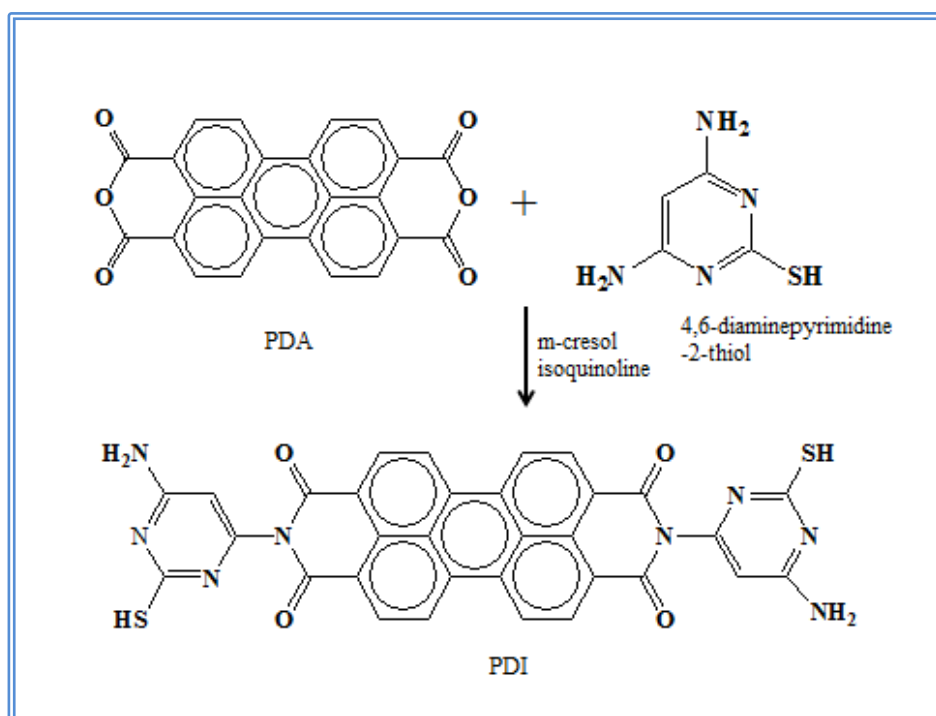
Elemental analysis were recorded using Carol-Erba 1106C, H and N analyser.

Differential scanning calorimetry analysis were recorded using a Perkin Elmer, Jade DSC instrument at  $10^{\circ}\text{C min}^{-1}$  in the presence of nitrogen.

Thermogravimetric thermograms were recorded using a Perkin Elmer. TGA mode, Pyris 1 at  $10^{\circ}\text{C min}^{-1}$  in oxygen.

### 3.3 Method of Synthesis

A new PDI (T-PDI) with metal binding potential is synthesized in this research work. The reaction occurs in one step via condensation of 4,6-diaminepyrimidine-2-thiol and perylene-3,4,9,10-tetracarboxylic dianhydride (PDA) using isoquinoline/*m*-cresol solvent mixture as shown in Scheme 3.1.



Scheme 3.1: Synthesis of T-PDI

### 3.4 Synthesis of T-PDI

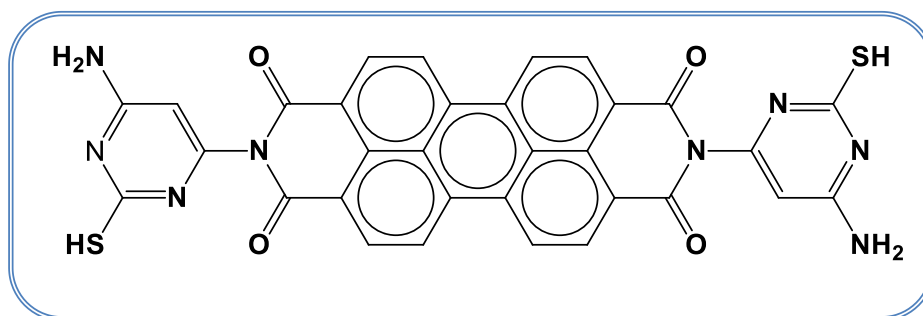


Figure 3.1. Structure of T-PDI

A mixture of 1.00 g (2.55 mmol) perylene-3,4,9,10-tetracarboxylic acid dianhydride, 1.4 g (10.20 mmol) of 4,6-diaminopyrimidine-2-thiol and 0.85 g (2.50 mmol) of zinc acetate were carefully heated in a solvent mixture (40 mL m-cresol and 40 mL isoquinoline) under argon gas at 100 °C for 2 hours. The reaction mixture was again heated for 4 hours at 150 °C. The temperature was further increased to 170 °C and 180 °C for 2 hours and 18 hours respectively. The solution was finally subjected to 200 °C for 5 hours.

The solution was kept to cool and was poured into 300 mL methanol for precipitation. The solution is subsequently filtered off by vacuum filtration, then purified with a Soxhlet apparatus for 40 hours to remove excess reactants and solvents with high boiling points. The purified product solution was dried under vacuum at 100°C.

**Yield:** 70%

**Colour of product:** Dark red



**IR: (KBr, cm<sup>-1</sup>):**  $\nu = 3400, 3092, 1697, 1645, 1585, 1535, 1402, 1330, 1253, 1174, 1120, 979, 806.$

**UV vis (DMF) ( $\lambda_{\max}$ , nm):** 462, 492, 528.

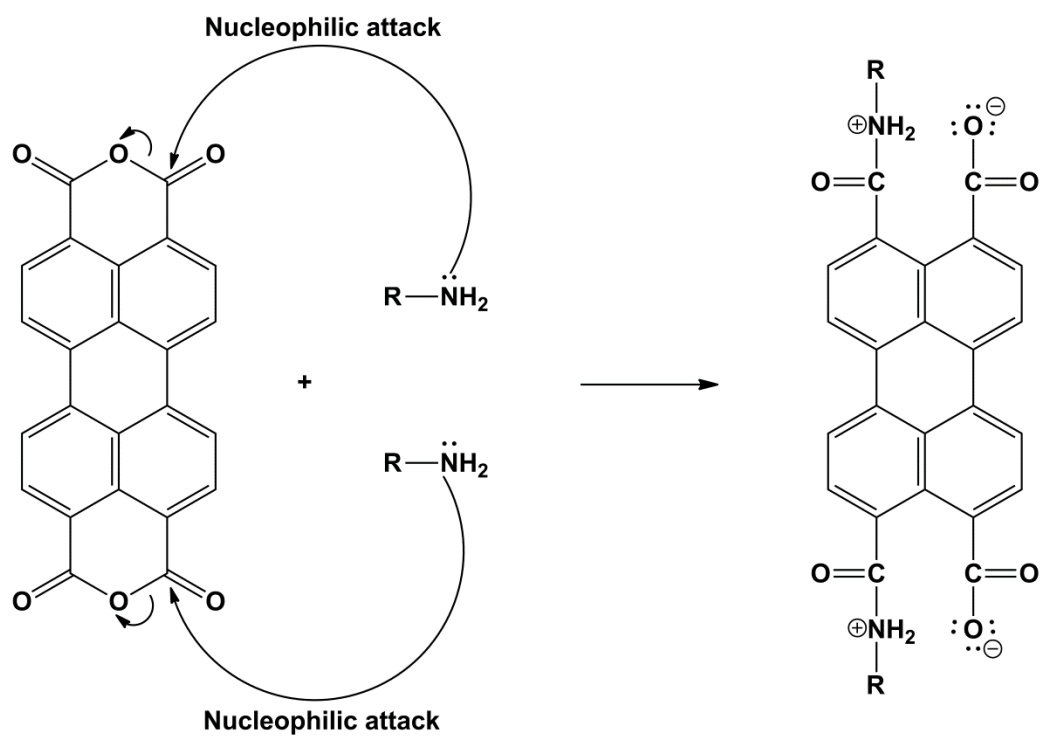
**Fluorescence (DMF)  $\lambda_{\max}$ , nm:** 543, 578, 630.

**Anal. Calcd. For (C<sub>32</sub>H<sub>16</sub>N<sub>8</sub>O<sub>4</sub>S<sub>2</sub>)<sub>n</sub> (Mw, (640.65g/mol)<sub>n</sub>):** C, 59.99%; H, 2.52%; N, 17.49%; S, 10.01%; O, 9.99%

**Found:** C, 58.95%; H, 2.42%; N, 16.95%; S, 9.29%;

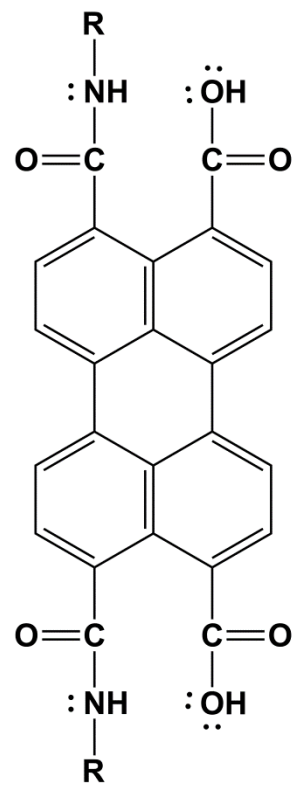
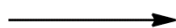
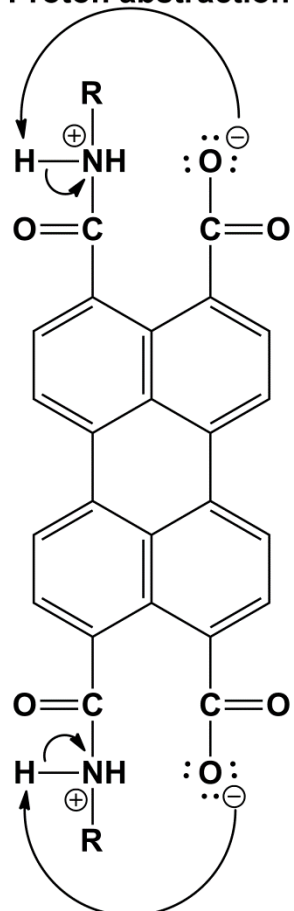
### 3.5 General Synthetic Mechanism of Perylene Dyes

#### STEP 1

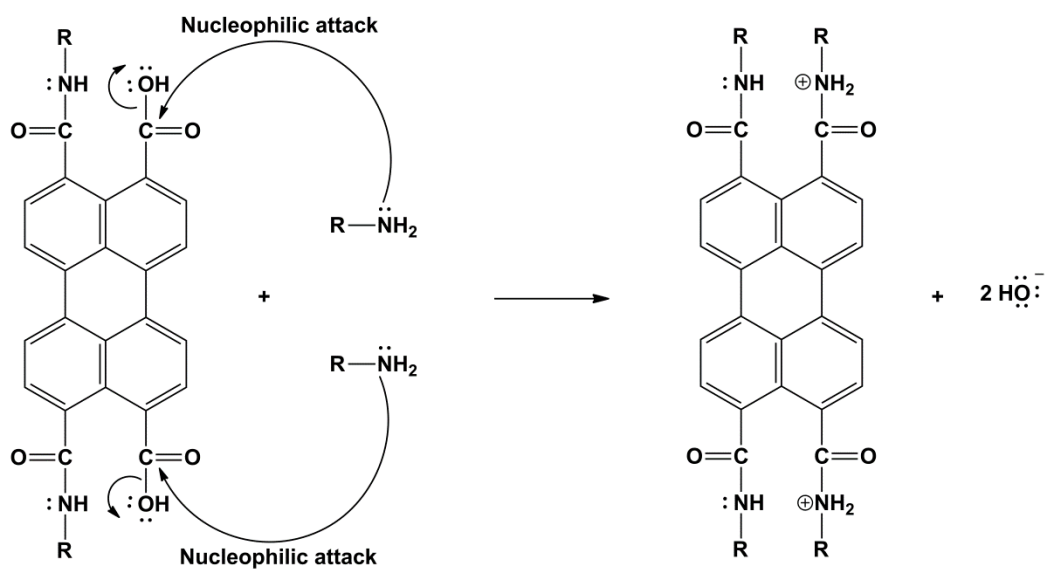


## STEP 2

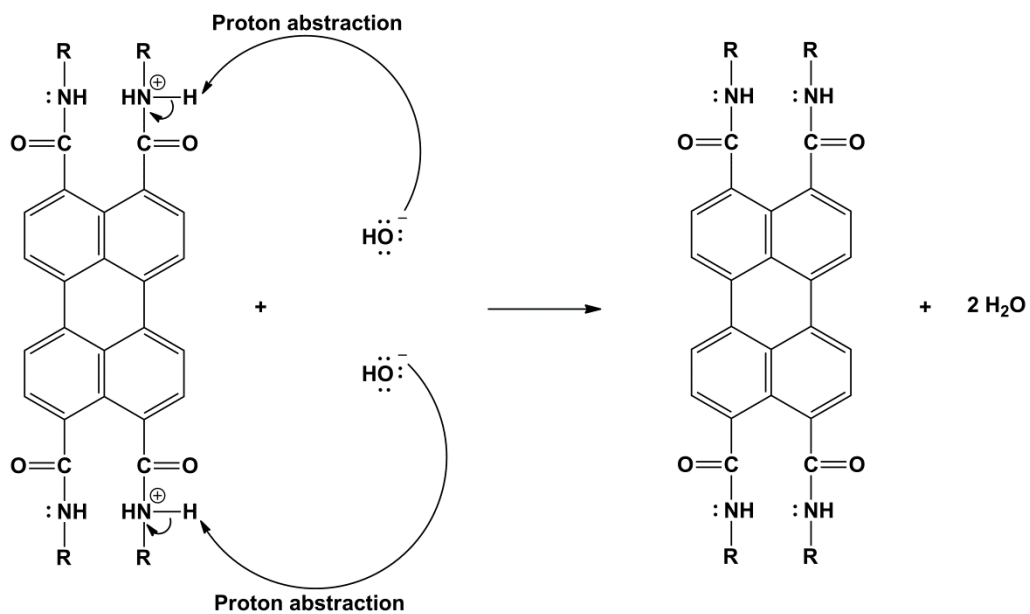
Proton abstraction



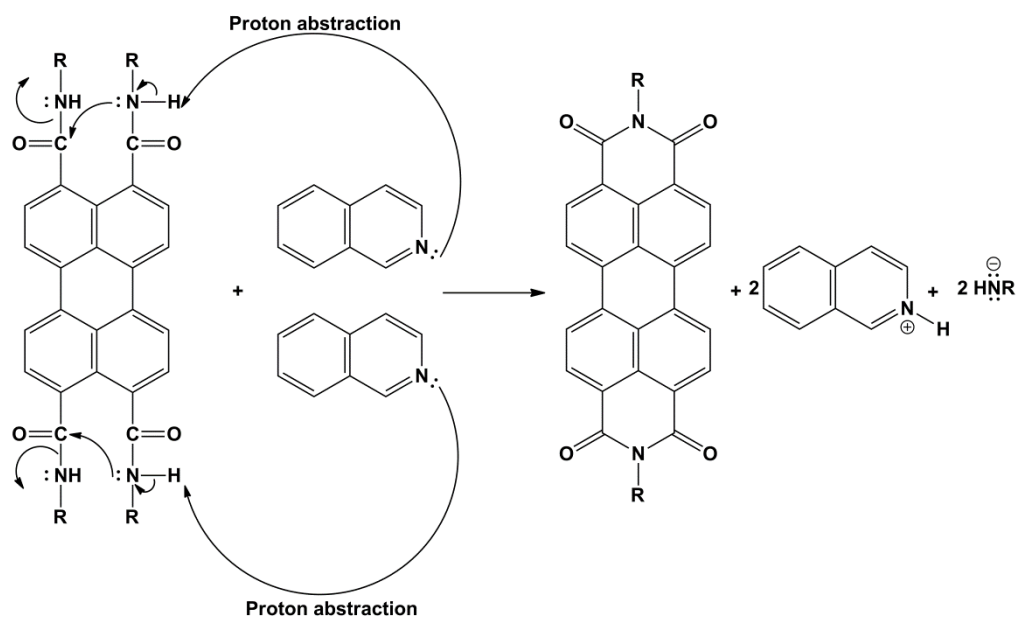
### STEP 3



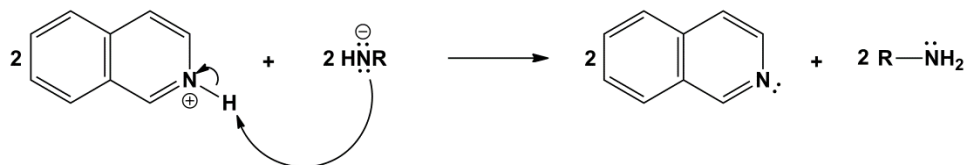
### STEP 4



## STEP 5



## STEP 6



## Chapter 4

### DATA AND CALCULATION

#### 4.1 Optical and Photochemical Properties

##### 4.1.1 Molar Absorption Coefficient ( $\epsilon_{max}$ )

Molar absorption coefficient is a measure of how strong a chemical specie absorbs light at a particular wavelength per molar concentration. It can be deduced from Beer Lambert's law (Equ 4.1)

$$\epsilon_{max} = \frac{A}{cl} \quad \text{Equ. (4.1)}$$

Where,

$\epsilon_{max}$  = molar extinction coefficient ( $\text{L}\cdot\text{mol}^{-1}\cdot\text{cm}^{-1}$ )

A = absorption of analyte at a wavelength

c = concentration of solution in ( $\text{mol}\cdot\text{L}^{-1}$ )

l = pathlength (cm)

At the wavelength,  $\lambda_{max} = 533\text{nm}$ , concentration =  $1 \times 10^{-5}\text{M}$  and absorption = 0.9

$$\epsilon_{max} = \frac{A}{cl} = \frac{0.9}{1 \times 10^{-5} \times 1}$$

$\epsilon_{max}$  of T – PDI in DMF =  $90,000 \text{ L}\cdot\text{mol}^{-1}\cdot\text{cm}^{-1}$

Table 4.1. Molar Absorptivity Data of T-PDI in TFA,DMF and NMP

Compound	Concentration (M)	Absorbance	$\lambda_{max}$	$\epsilon_{max}$ ( $\text{LM}^{-1}\text{cm}^{-1}$ )
DMF	$1 \times 10^{-5}$	0.9	528	90000
NMP	$1 \times 10^{-5}$	0.8	527	80000
TFA	$1 \times 10^{-5}$	1.1	533	110000

#### 4.1.2 Fluorescence Quantum Yield ( $\phi_f$ )

A chromophore or fluorophore absorbs photons of light (energy) for the formation of an energetic excited state. This gives rise to a deactivation process such as fluorescence, internal conversion, intersystem crossing and vibrational relaxation etc. it is usually represented by the Jablonski diagram (Figure 4.1).

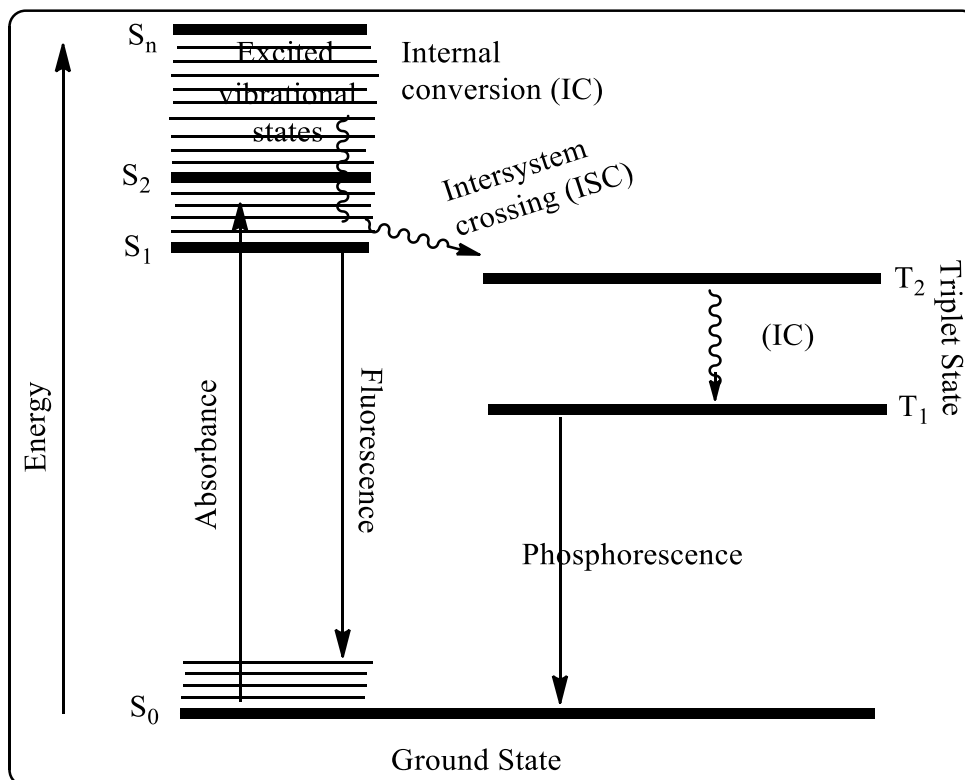


Figure 4.1: Jablonski Diagram

Therefore, the ratio of photons absorbed to the photons emitted is known as

Fluorescence Quantum Yield ( $\Phi_f$ )

$$\Phi_u = \frac{A_{std}}{A_u} \times \frac{S_u}{S_{std}} \times \left(\frac{n_u}{n_{std}}\right)^2 \times \Phi_{std} \quad \text{Equ (4.2)}$$

Where,

$\Phi_u$  : Fluorescence quantum yield of unknown

$A_{std}$ : Absorbance of the reference at the excitation wavelength

$A_u$  : Absorbance of the unknown at the excitation wavelength

$S_{std}$ : The integrated emission area across the band of reference

$S_u$  : The integrated emission area across the band of unknown

$n_{std}$ : Refractive index of reference solvent

$n_u$  : Refractive index of unknown solvent

$\Phi_{std}$ : Fluorescence quantum yield of reference.

The N,N'-bis(dodecyl)-3,4,9,10-perylenebis(dicarboximide) ( $\Phi_f = 1$ ) (Icil, 1996) was used as reference in chloroform for the fluorescence quantum yield measurements of T-PDI. The excitation wavelength,  $\lambda_{exc}$  of both T-PDI and reference was 485 nm.

### Fluorescence Quantum Yield of T-PDI in DMF

$A_{std}(dodecyl) = 0.1003$ ,  $A_u = 0.1008$ ,  $S_{std} = 851.81$   $S_u = 67.18$ ,  $n_{std} = 1.4458$ ,  
 $n_u = 1.4305$ ,  $\Phi_{std} = 1$

$$\Phi_u = \frac{0.1003}{0.1008} \times \frac{67.18}{851.81} \times \left(\frac{1.4305}{1.4458}\right)^2 \times 1$$

$$\Phi_u = \mathbf{0.08}$$



## Fluorescence Quantum Yield of T-PDI in NMP

$$A_{std}(dodecyl) = 0.1003, A_u = 0.1006, S_{std} = 851.81, S_u = 49.79, n_{std} = 1.4458,$$

$$n_u = 1.47, \phi_{std} = 1$$

$$\phi_u = \frac{0.1003}{0.1006} \times \frac{49.79}{851.81} \times \left(\frac{1.4700}{1.4458}\right)^2 \times 1$$

$$\phi_u = 0.06$$

### 4.1.3 Half Width of the Selected Absorption Band ( $\Delta\bar{\nu}_{1/2}$ )

The half width of the absorption band can be calculated by the equation

$$\Delta\bar{\nu}_{1/2} = \bar{\nu}_1 - \bar{\nu}_2$$

Equ (4.3)

Where,

$\Delta\bar{\nu}_{1/2}$  = Half width of the selected absorption maximum in  $\text{cm}^{-1}$

$\bar{\nu}_1 - \bar{\nu}_2$  = the estimated frequencies from the absorption of compound in  $\text{cm}^{-1}$

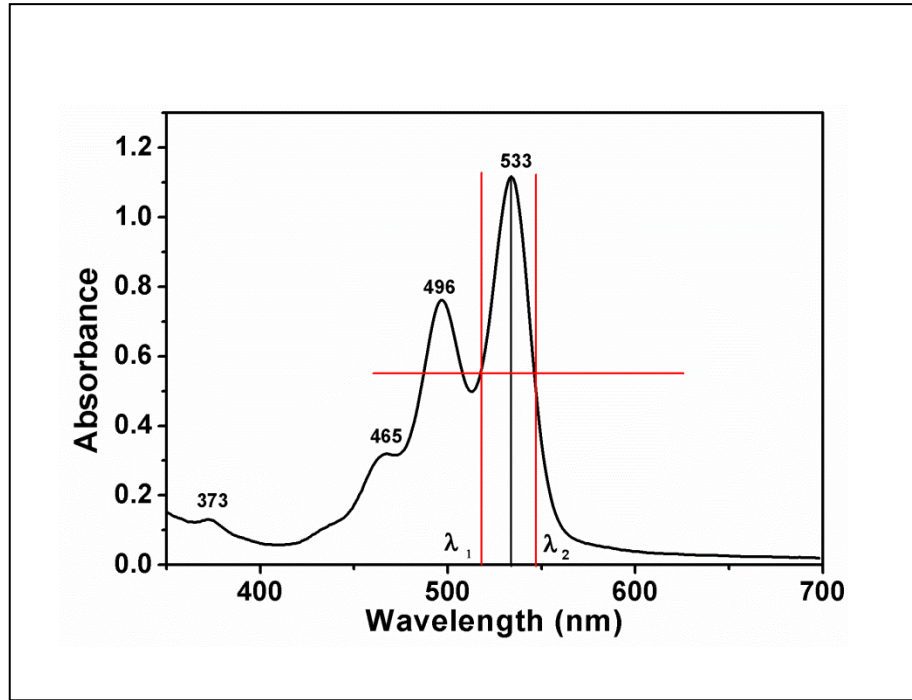


Figure 4.2. Representative Half-Width Plot on the Absorption Spectrum of T-PDI in TFA

From Figure 4.2,  $\lambda_1 = 526 \text{ nm}$

$$\lambda_1 = 526 \times \frac{10^{-9}m}{1nm} \times \frac{1cm}{10^{-2}m} = 5.26 \times 10^{-5}cm$$

$$\nu_1 = \frac{1}{5.26 \times 10^{-5}cm} = 19011.4 \text{ cm}^{-1}$$

Also from Figure 4.2,  $\lambda_2 = 542 \text{ nm}$

$$\lambda_2 = 542 \times \frac{10^{-9}m}{1nm} \times \frac{1cm}{10^{-2}m} = 5.42 \times 10^{-5}cm$$

$$\nu_2 = \frac{1}{5.42 \times 10^{-5}cm} = 18450.2 \text{ cm}^{-1}$$

$$\Delta\bar{\nu}_{1/2} = \bar{\nu}_1 - \bar{\nu}_2 = 19011.4 \text{ cm}^{-1} - 18450.2 \text{ cm}^{-1} = 561.2 \text{ cm}^{-1}$$

$$\Delta\bar{\nu}_{1/2} = 561.2 \text{ cm}^{-1}$$

In a similar method, the half- width of T-PDI for different solvents was estimated as shown in Table 4.2.

Table 4.2: Half width of T-PDI in different solvents.

Solvents	$\lambda_1, \lambda_2$ (nm)	$\bar{\nu}_1$ (cm <sup>-1</sup> ), $\bar{\nu}_2$ (cm <sup>-1</sup> )	$\Delta\bar{\nu}_{1/2}$ (cm <sup>-1</sup> )
<b>DMF</b>	521, 537	19193.9, 18621.97	571.93
<b>NMP</b>	520, 540	19230.8, 18518.5	712.30
<b>TFA</b>	526, 542	19011.4, 18450.2	561.20

#### 4.1.4 Theoretical Radiative Lifetime ( $\tau_0$ )

When the lifetime of an excited molecule is measured in the absence of radiationless transitions, it is usually referred to as theoretical radiative lifetime. Equation 4.4 will be used to deduce this value.

$$\tau_0 = \frac{3.5 \times 10^8}{\bar{\nu}_{max}^2 \times \epsilon_{max} \times \Delta\bar{\nu}_{1/2}} \quad \text{Equ (4.4)}$$

Where  $\tau_0$  = theoretical radiative lifetime in ns

$\bar{\nu}_{max}$  = mean frequency of the maximum absorption band in cm<sup>-1</sup>

$\epsilon_{max}$  = maximum absorption coefficient in L. mol<sup>-1</sup>. cm<sup>-1</sup>

$\Delta\bar{\nu}_{1/2}$  = Half width of the selected absorption in cm<sup>-1</sup>

The Theoretical Radiative Lifetime of T-PDI in TFA is calculated as follows using the values of molar absorptivity and half-width of selected absorption:

From Figure 4.1.and 4.2,  $\lambda_{max} = 533 \text{ nm}$

$$\lambda_{max} = 533 \times \frac{10^{-9}m}{1nm} \times \frac{1cm}{10^{-2}m} = 5.33 \times 10^{-5}cm$$

$$\nu_{max} = \frac{1}{5.33 \times 10^{-5}cm} = 18761.7cm^{-1}$$

$$\nu_{max}^2 = 3.52 \times 10^8 (cm^{-1})^2$$

$$\tau_0 = \frac{3.5 \times 10^8}{3.52 \times 10^8 \times 110000 \times 561.2} = 1.611 \times 10^{-8}s$$

$$\tau_0 = 1.611 \times 10^{-8}s \times \frac{1ns}{10^{-9}s}$$

$$\tau_0 = 16.11 \text{ ns}$$

Similar calculations were done for the same compound but in other solvents, represented in Table 4.3.

Table 4.3. Theoretical radiative lifetime of T-PDI in different solvents

Solvents	$\lambda_{max}(nm)$	$\epsilon_{max}(M^{-1}cm^{-1})$	$\nu_{max}^2(cm^{-1})^2$	$\Delta\nu_{1/2}cm^{-1}$	$\tau_0(ns)$
<b>DMF</b>	528	90000	$3.59 \times 10^8$	571.93	18.94
<b>NMP</b>	527	80000	$3.60 \times 10^8$	712.30	17.06
<b>TFA</b>	533	110000	$3.52 \times 10^8$	561.20	16.11

#### 4.1.5 Theoretical Fluorescence Life Time ( $\tau_f$ )

This is the theoretical average time a molecule remains in the excited state just before photons are emitted (fluorescence), (Turro, 1965). usually represented as

$$\tau_f = \tau_0 \times \phi_f \quad \text{Equ (4.5)}$$

Where  $\tau_f$  = fluorescence lifetime (ns)

$\tau_0$  = theoretical radiative lifetime (ns)

$\phi_f$  = fluorescence quantum yield

The theoretical fluorescence lifetime of T-PDI in DMF is calculated as follows using values of theoretical radiative lifetime and fluorescence quantum yield.

$$\tau_f = 18.94 \times 0.076$$

$$\tau_f = 1.45$$

Table 4.4. Theoretical fluorescence lifetime ( $\tau_f$ ) of T-PDI in different solvents

Solvents	$\tau_0$	$\phi_f$	$\tau_f$
DMF	18.94	0.076	1.45
NMP	17.06	0.06	1.02

#### 4.1.6 Fluorescence Rate Constants ( $k_f$ )

The Fluorescence Rate Constant for T-PDI was calculated by the following equation. (Turro, 1965).

$$k_f = \frac{1}{\tau_0} \quad \text{Equ (4.6)}$$

Where  $k_f$  = fluorescence rate constant in  $s^{-1}$

$\tau_0$  = theoretical radiative lifetime in s

Thus, the fluorescence rate constant for T-PDI in TFA is calculated accordingly

$$k_f = \frac{1}{\tau_0} = \frac{1}{16.11 \times 10^{-9}} = 6.21 \times 10^7 \text{ s}^{-1}$$

$$k_f = 6.21 \times 10^7 \text{ s}^{-1}$$

Table 4.5. Fluorescence rate constants of T-PDI in different solvents

Solvents	$\tau_0$ (ns)	$k_f$ ( $\text{s}^{-1}$ )
DMF	18.94	$5.28 \times 10^7$
NMP	17.06	$5.86 \times 10^7$
TFA	16.21	$6.21 \times 10^7$

#### 4.1.7 Rate Constants of Radiationless Deactivation ( $k_d$ )

The rate constants of radiationless deactivations of the synthesized T-PDI compound is calculated by the equation

$$k_d = \left( \frac{k_f}{\phi_f} \right) - k_f \quad \text{Equ (4.7)}$$

Where  $k_d$  = the rate constant of radiationless deactivation in  $\text{s}^{-1}$

$k_f$  = fluorescence rate constant in  $\text{s}^{-1}$

$\phi_f$  = fluorescence quantum yield

The rate constants of radiationless deactivations of the synthesized T-PDI in DMF is calculated as follows

$$k_d = \left(\frac{k_f}{\phi_f}\right) - k_f$$

$$k_d = \left(\frac{5.28 \times 10^7}{0.0768}\right) - 5.28 \times 10^7$$

$$k_d = 6.347 \times 10^6$$

Table 4.6. Rate constants of radiationless deactivation ( $k_d$ ) of T-PDI in DMF and NMP

Solvents	$k_f$	$\phi_f$	$k_d$
DMF	$5.28 \times 10^7$	0.08	$635 \times 10^6$
NMP	$5.86 \times 10^7$	0.06	$918 \times 10^7$

#### 4.1.8 Oscillator Strength ( $f$ )

The oscillator strength expresses the strength of an electronic transition and its calculated by the following equation.

$$f = 4.32 \times 10^{-9} \times \Delta\bar{\nu}_{1/2} \epsilon_{\max}$$

Equ (4.8)

where  $f$  = oscillator strength

$\Delta\bar{\nu}_{1/2}$  = half width of the selected absorption in units of  $\text{cm}^{-1}$

$\epsilon_{\max}$  = maximum absorption coefficient in  $\text{L. mol}^{-1} \cdot \text{cm}^{-1}$

The oscillator strength of the synthesized T-PDI compound in TFA is calculated as follows

Where  $\Delta\bar{\nu}_{1/2}$  (TFA) =  $561.20 (\text{cm}^{-1})^2$ , and  $\epsilon_{\max}$  (TFA) =  $110000 \text{M}^{-1} \cdot \text{cm}^{-1}$

$$f = 4.32 \times 10^{-9} \times 561.20 \times 110000 = 0.27$$

$$f = 0.27$$

The oscillator strength of T-PDI in other solvents is summarized below Table 4.7.

Table 4.7. The oscillator strength of T-PDI in other solvents

Solvents	$\epsilon_{\max}$ ( $\text{M}^{-1}\text{cm}^{-1}$ )	$\Delta V_{1/2}$ ( $\text{cm}^{-1}$ ) <sup>2</sup>	$f$
DMF	90000	571.93	0.22
NMP	80000	712.30	0.25
TFA	110000	561.20	0.27

#### 4.1.9 Singlet energies ( $E_s$ )

Singlet energy is the minimum amount of energy required for a chromophore of fluorophore to get excited from ground state to an excited state.

$$E_s = \frac{2.86 \times 10^5}{\lambda_{\max}}$$

Equ (4.9)

Where  $E_s$  = singlet energy in kcal mol<sup>-1</sup>

$\lambda_{\max}$  = maximum absorption wavelength in Å

Singlet energy of T-PDI in TFA is shown below

Where  $\lambda_{\max}$  (TFA) = 533 nm

$$533 \text{ nm} \times \frac{10^{-9} \text{ m}}{1 \text{ nm}} \times \frac{1 \text{ \AA}}{10^{-10} \text{ m}} = 5330 \text{ \AA}$$

$$E_s = \frac{2.86 \times 10^5}{5330} = 53.7 \text{ kcal mol}^{-1}$$



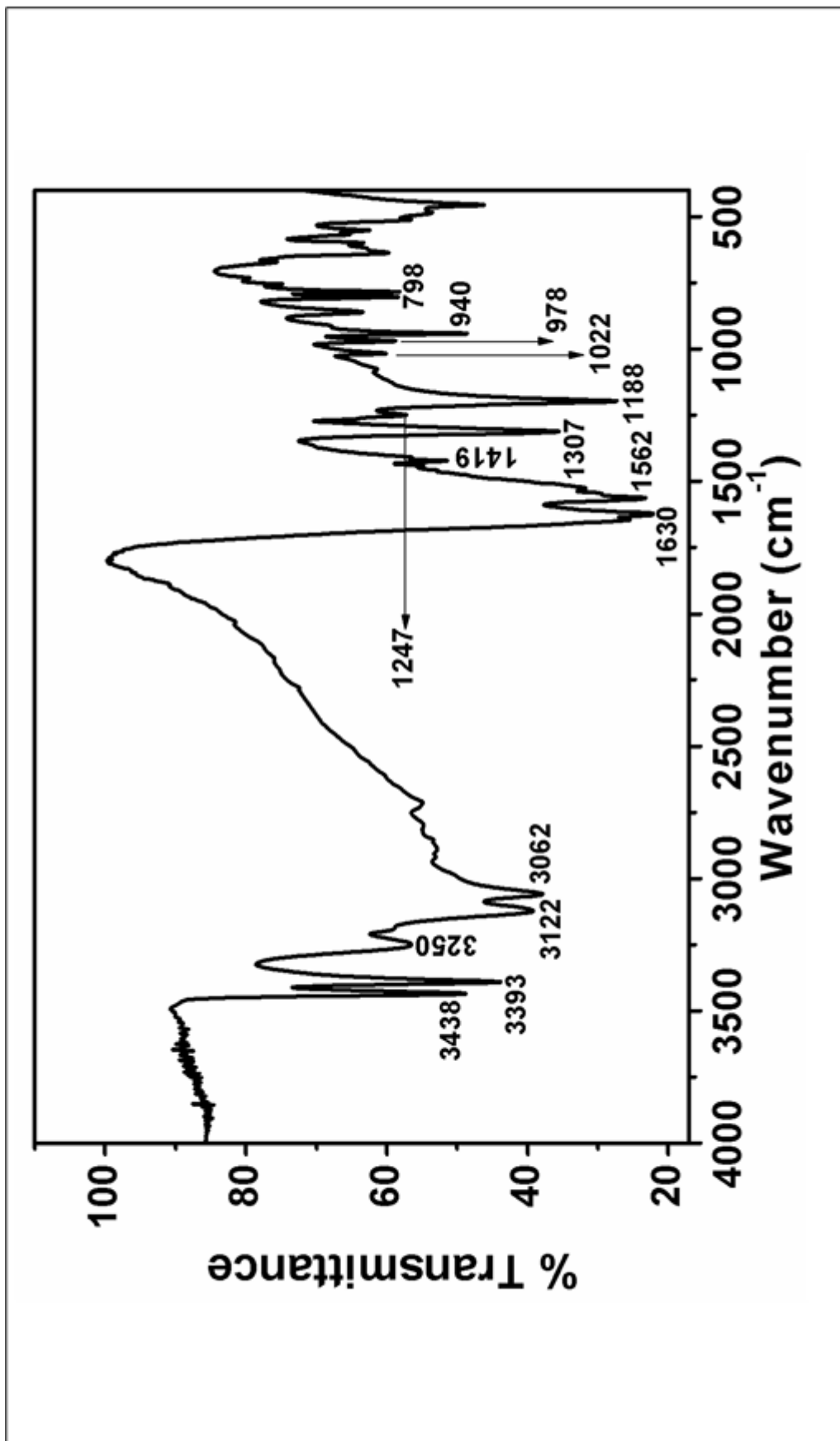
$$E_s = 53.7 \text{ kcal mol}^{-1}$$

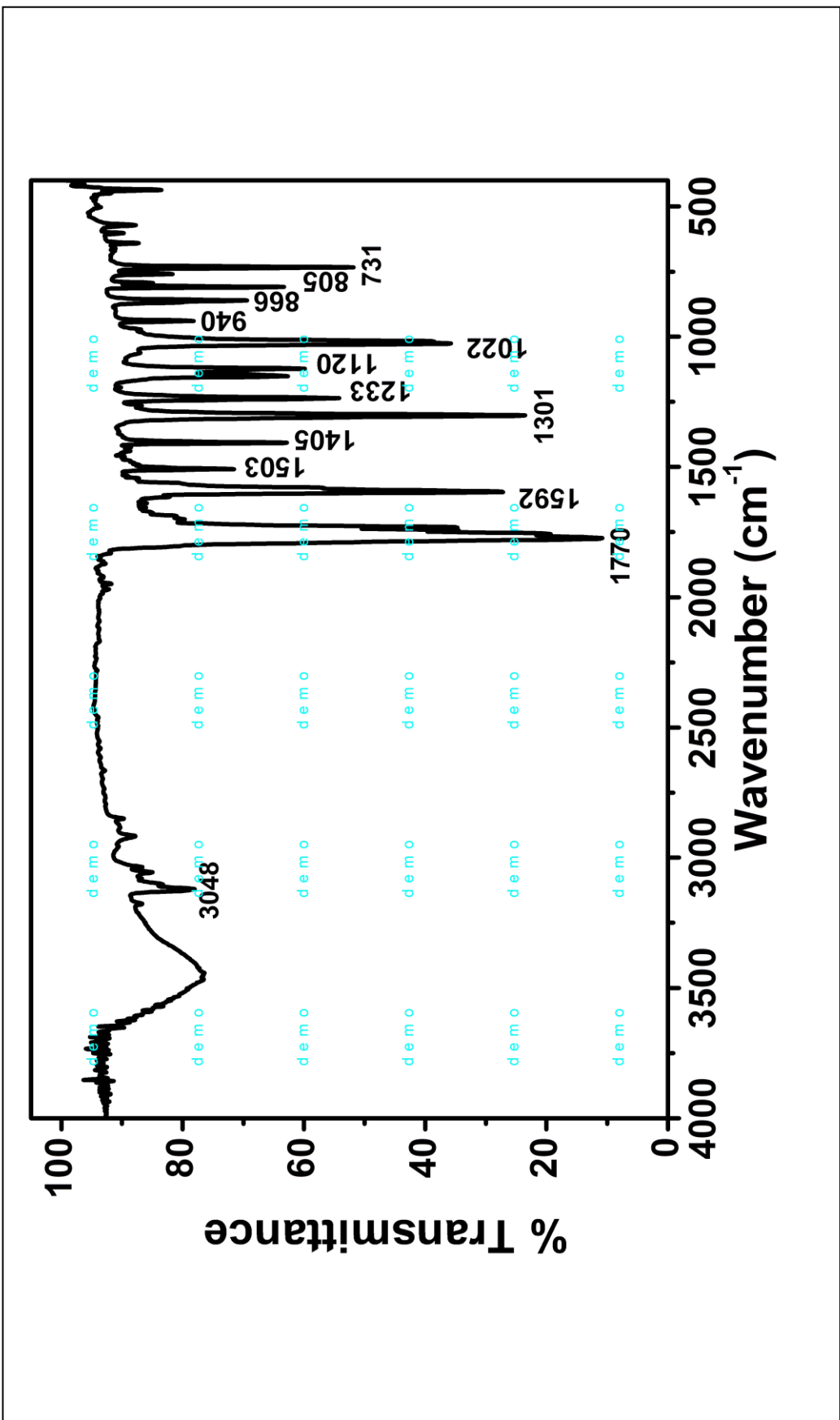
Table 4.8. Single energies of T-PDI in different solvents are summarized

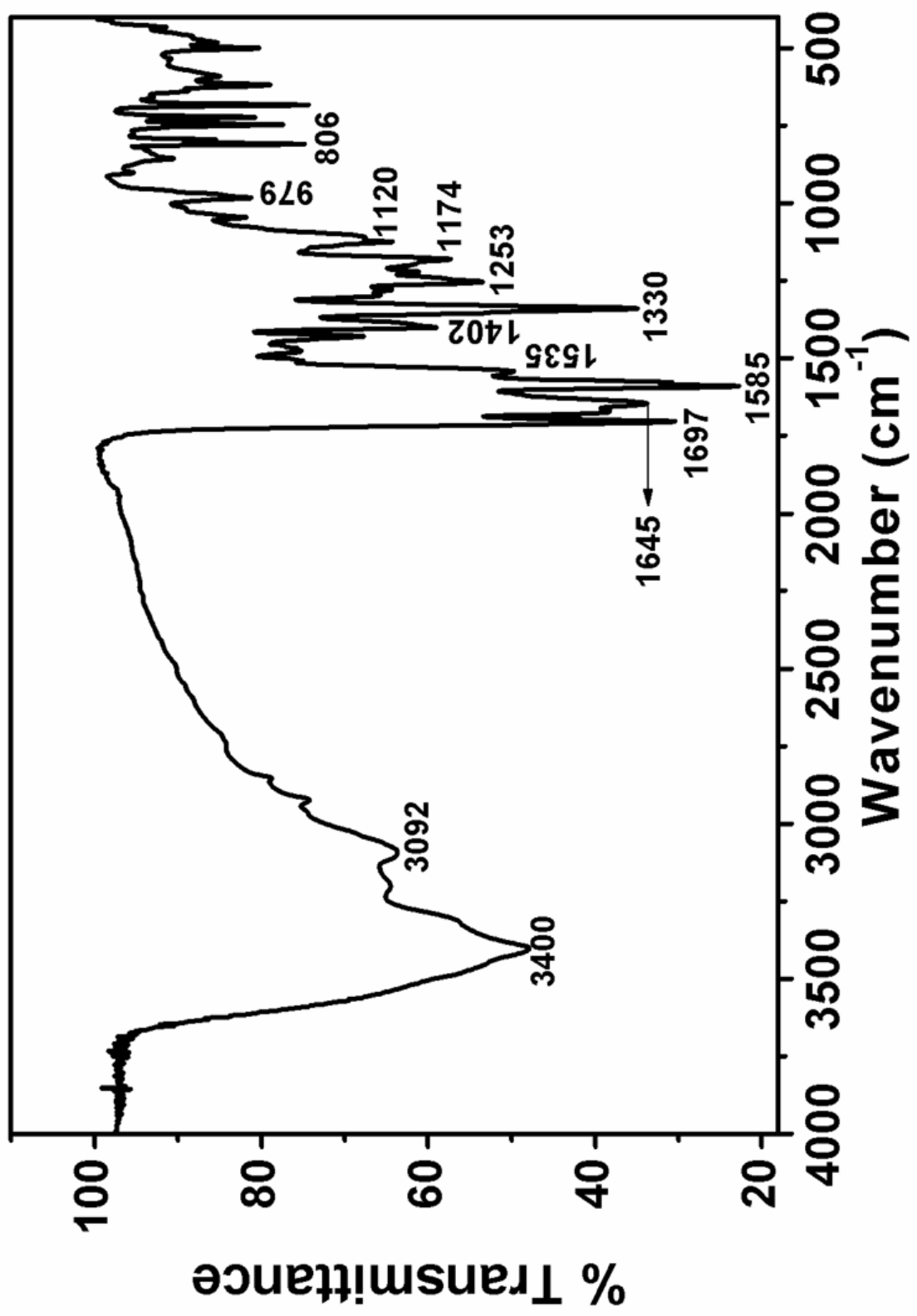
Solvents	$\lambda_{max}(\text{nm})$	$\lambda_{max}(\text{\AA})$	$E_s(\text{kcal mol}^{-1})$
DMF	528	5280	54.2
NMP	527	5270	54.3
TFA	533	5330	53.7

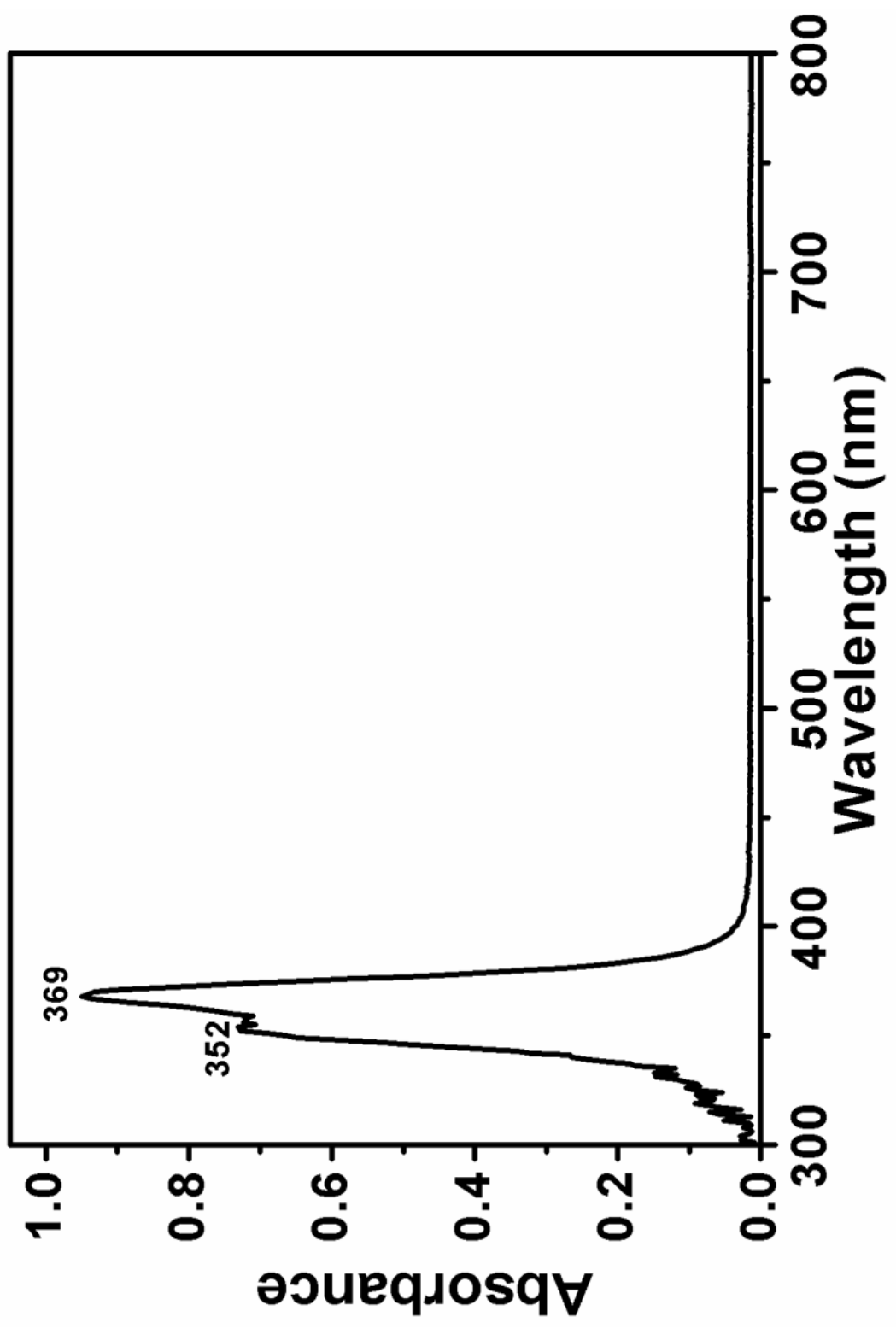
## 4.2 Thermal Properties

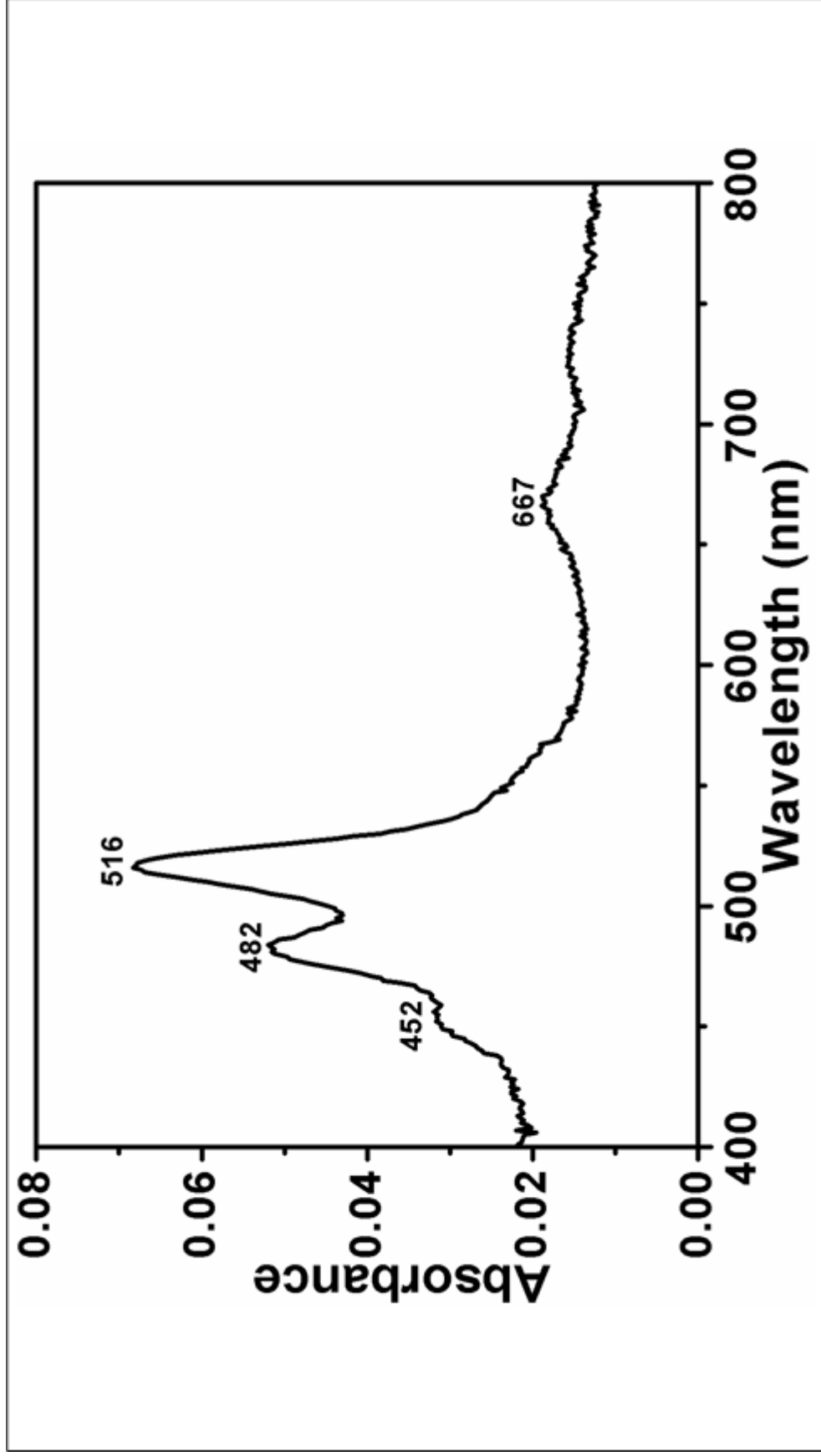
The thermal behavior of T-PDI was investigated by DSC (heating rate 10 K.min<sup>-1</sup>) and TGA (heating rate 5 K.min<sup>-1</sup>).

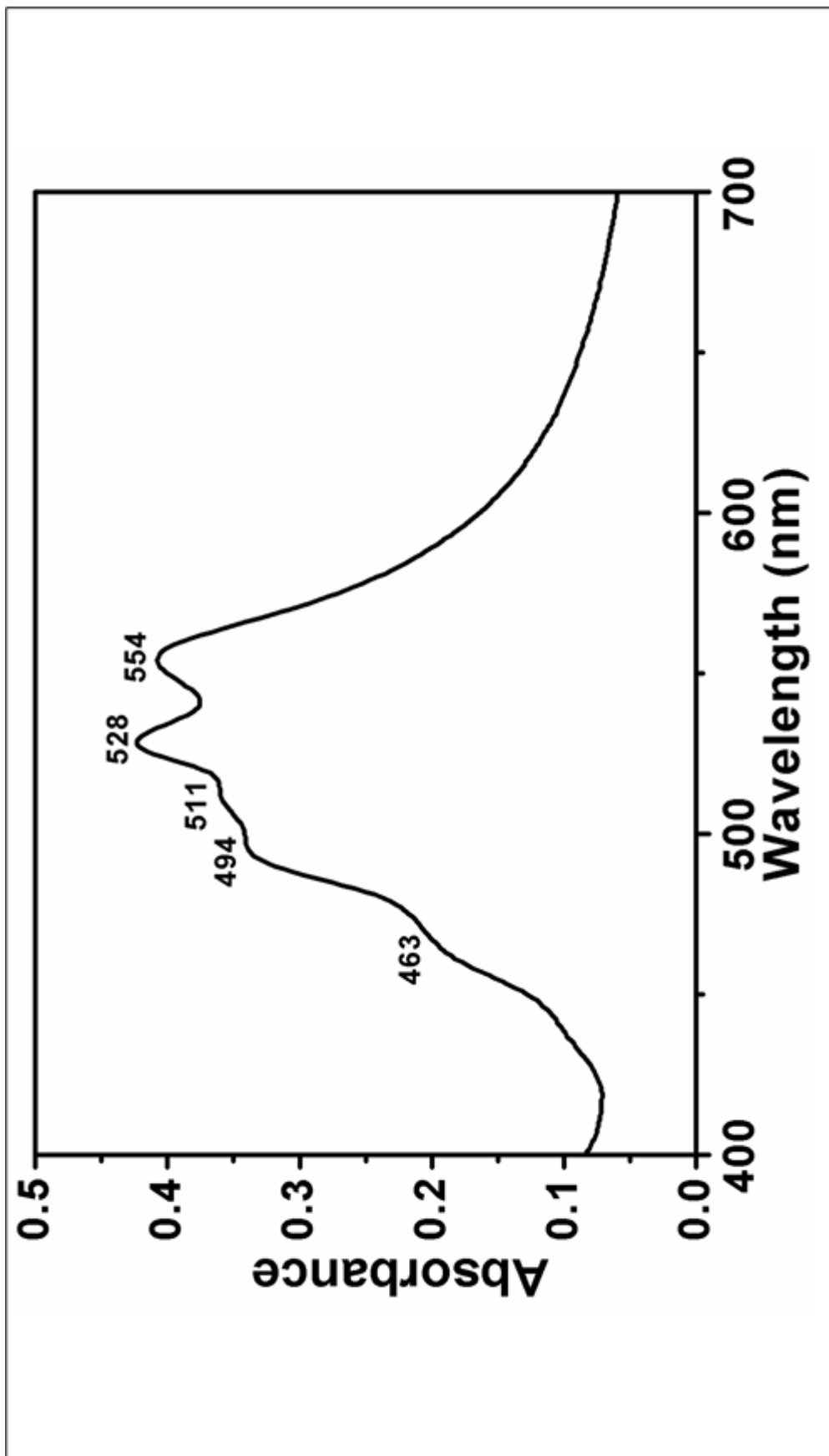


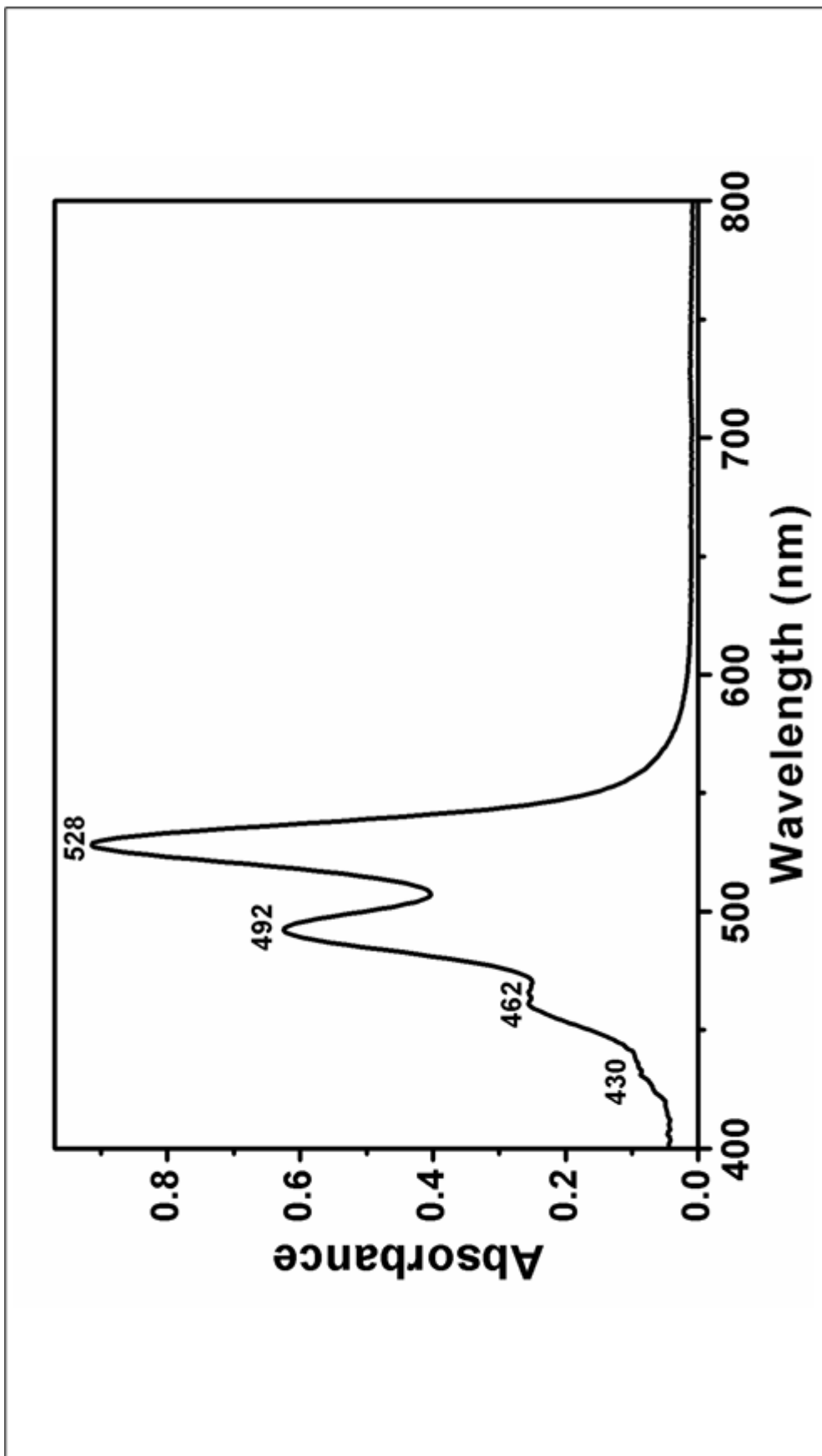




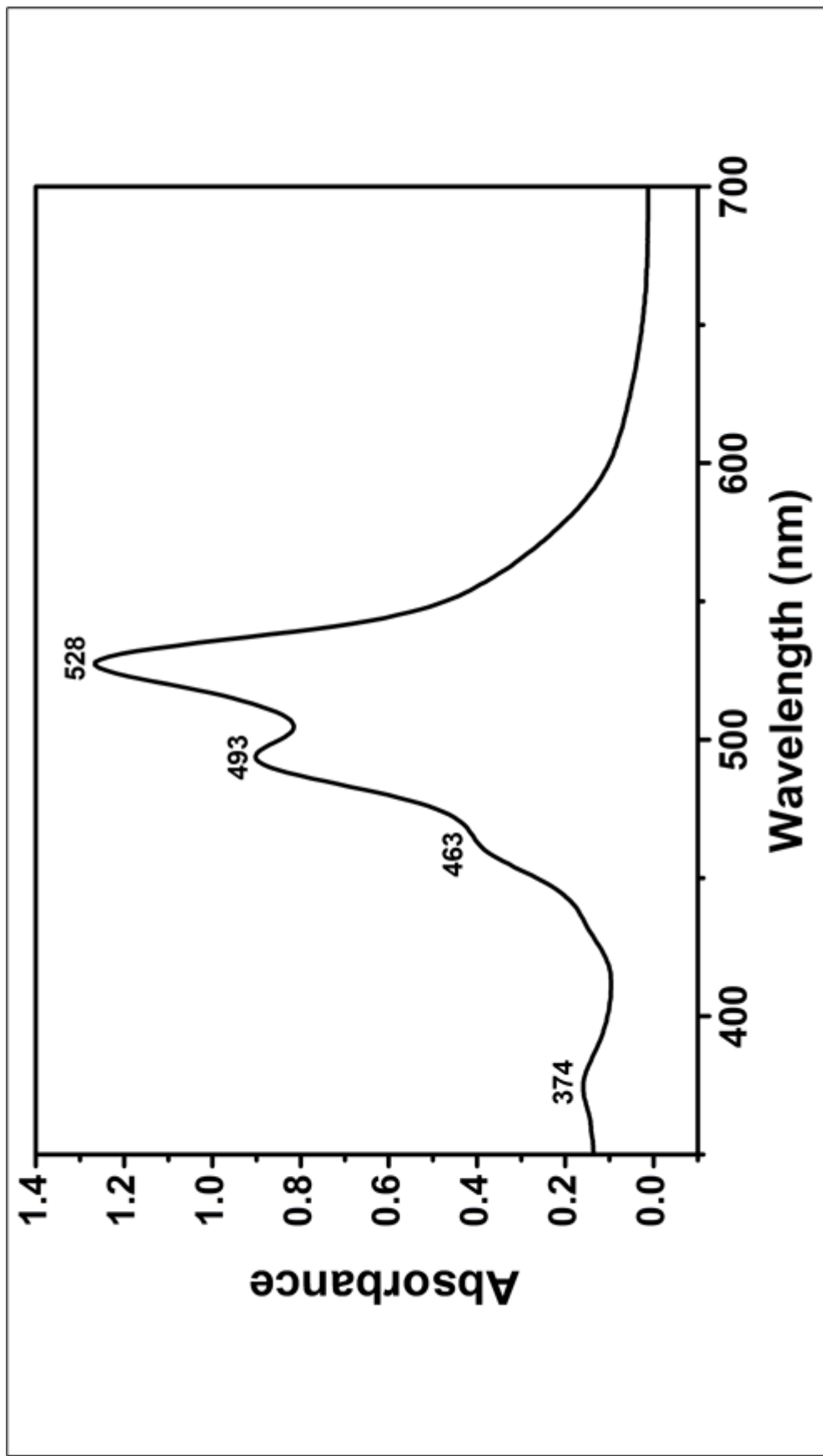


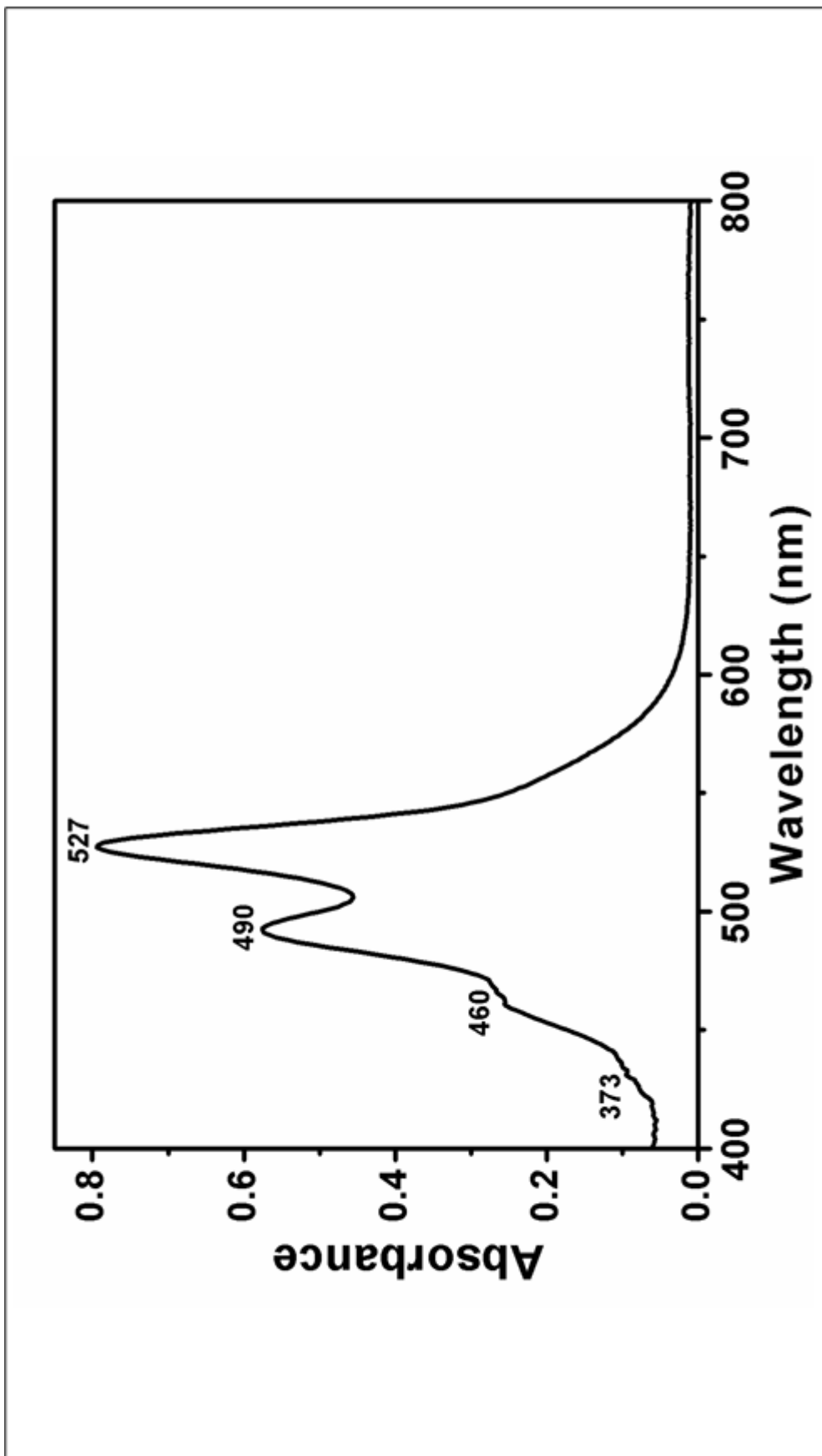


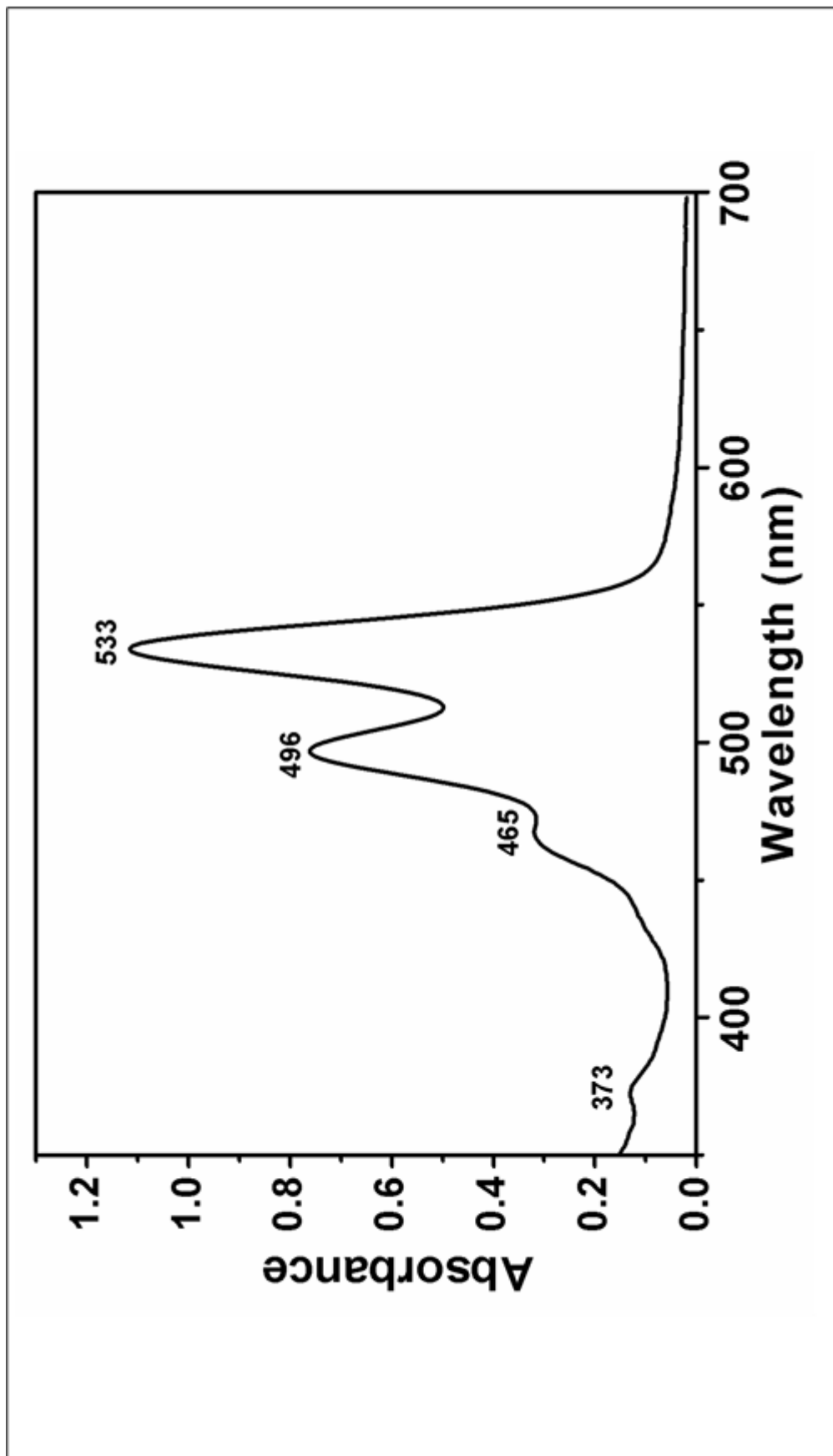


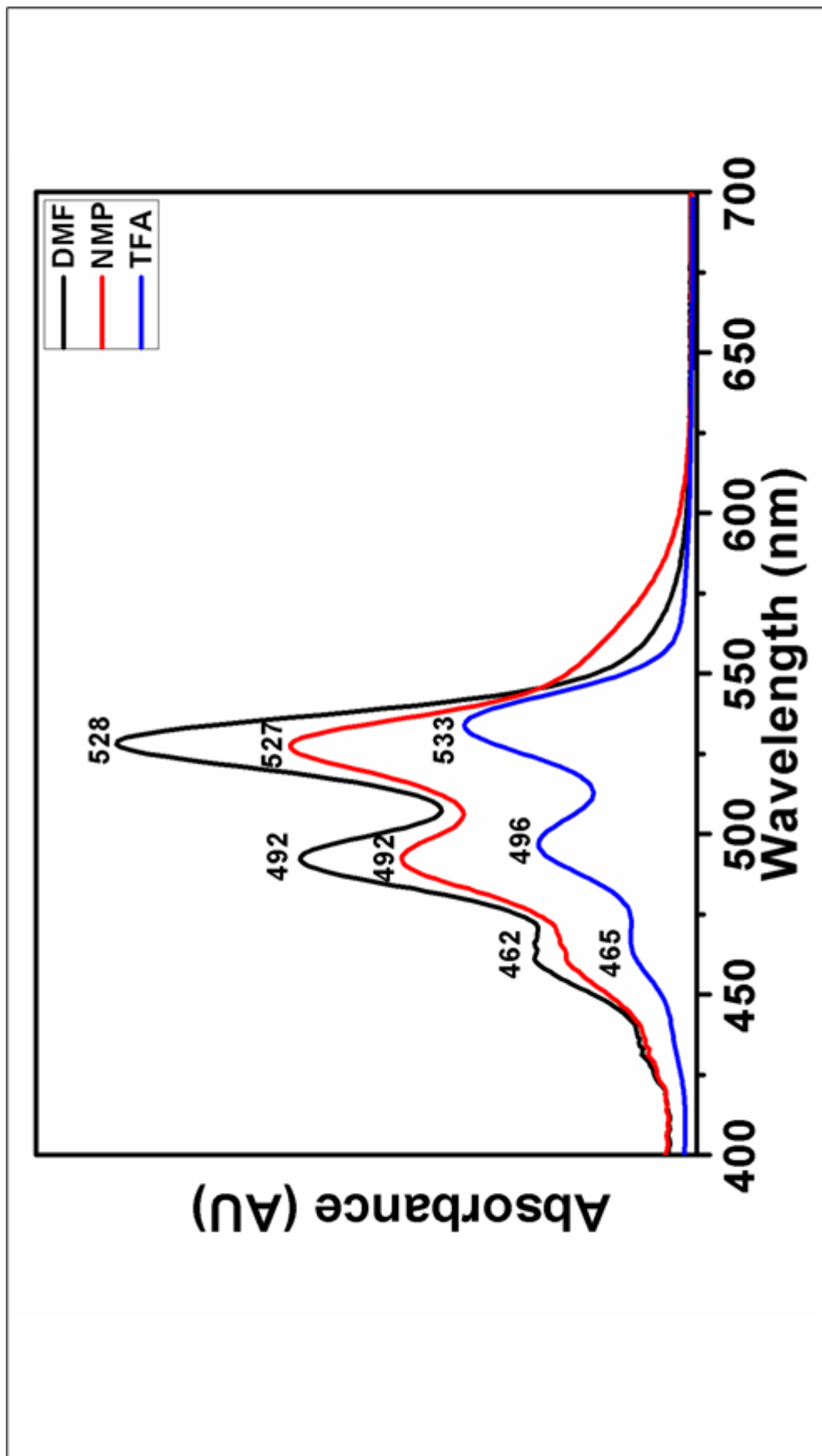


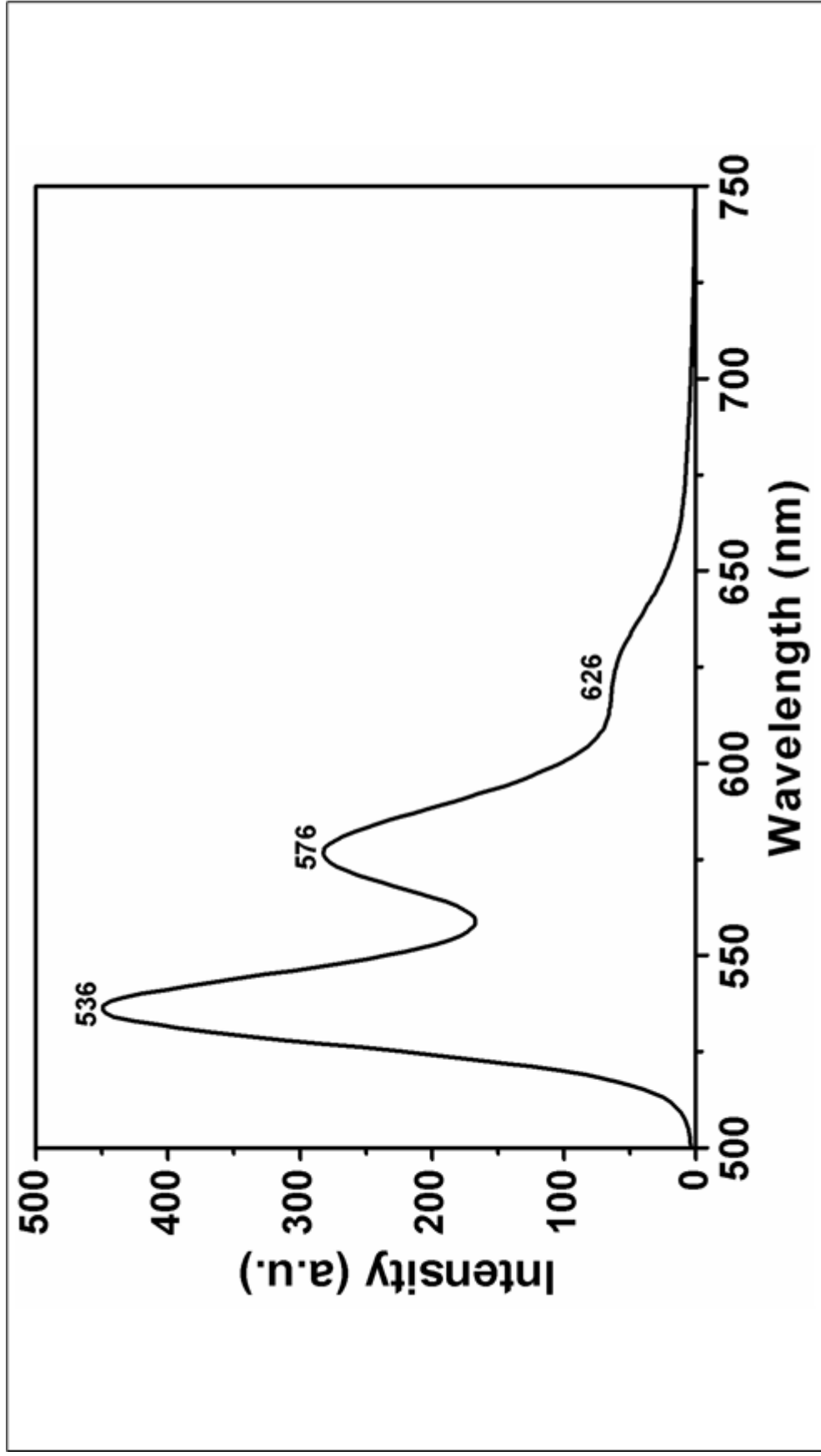


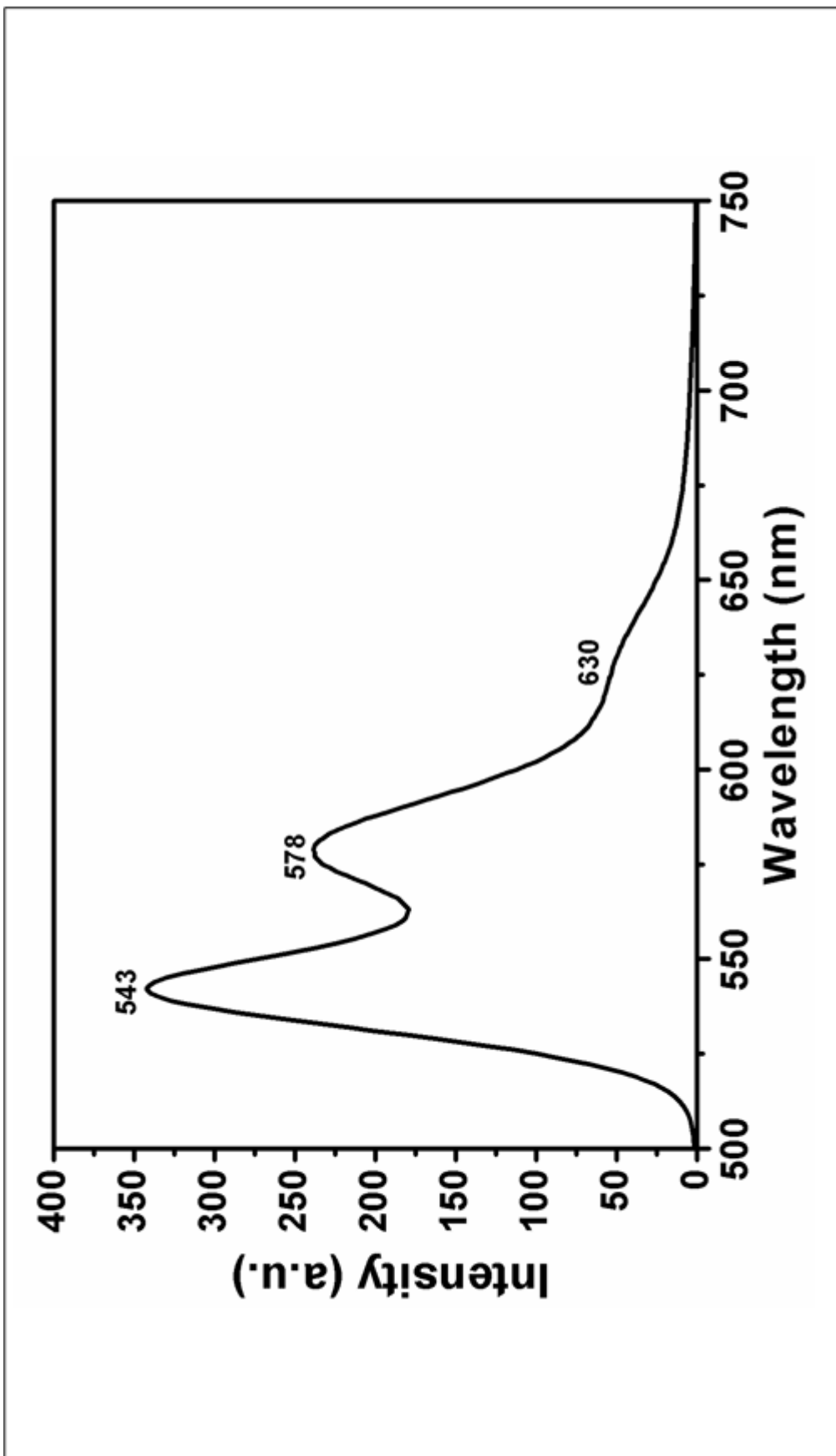


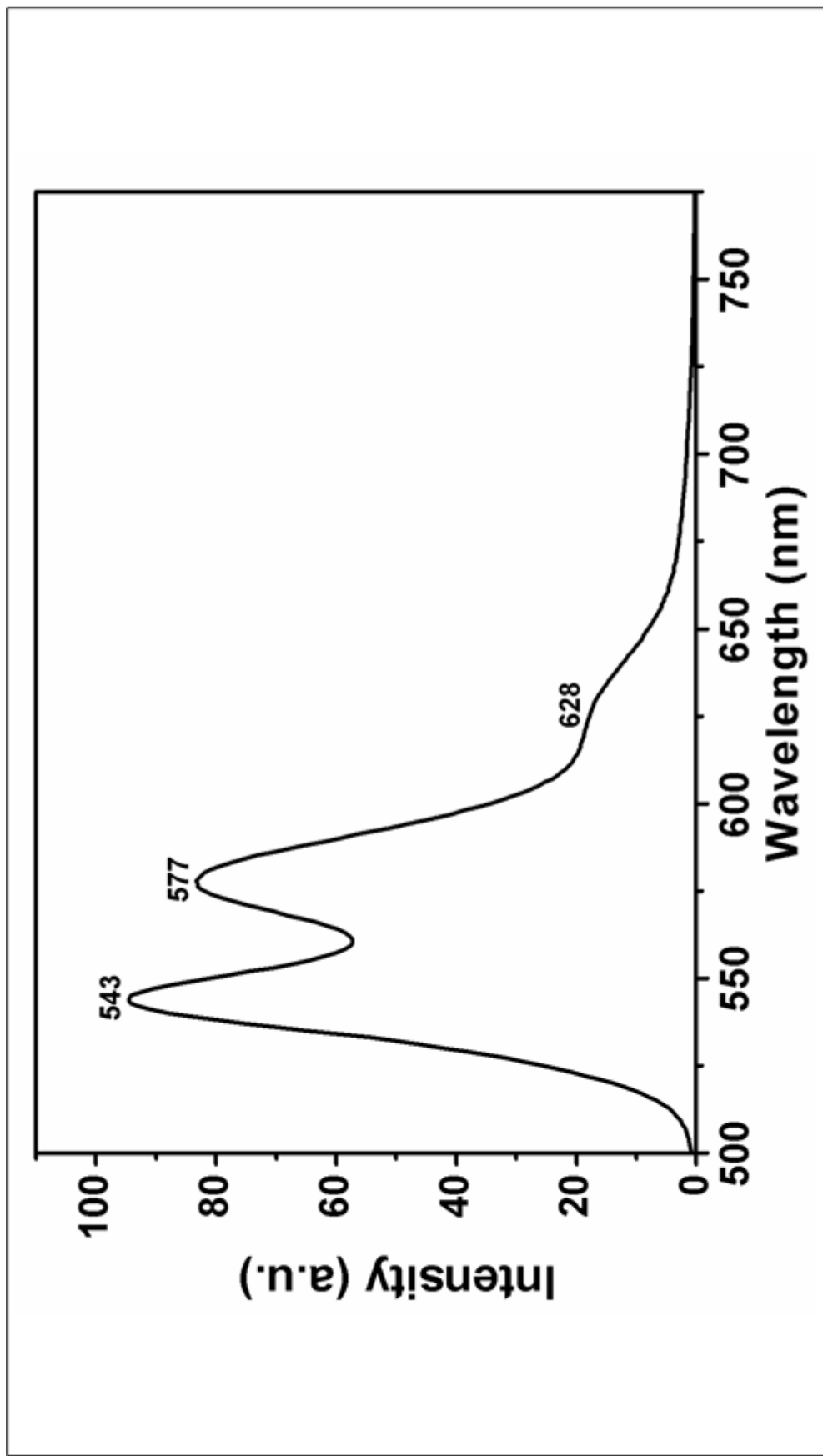


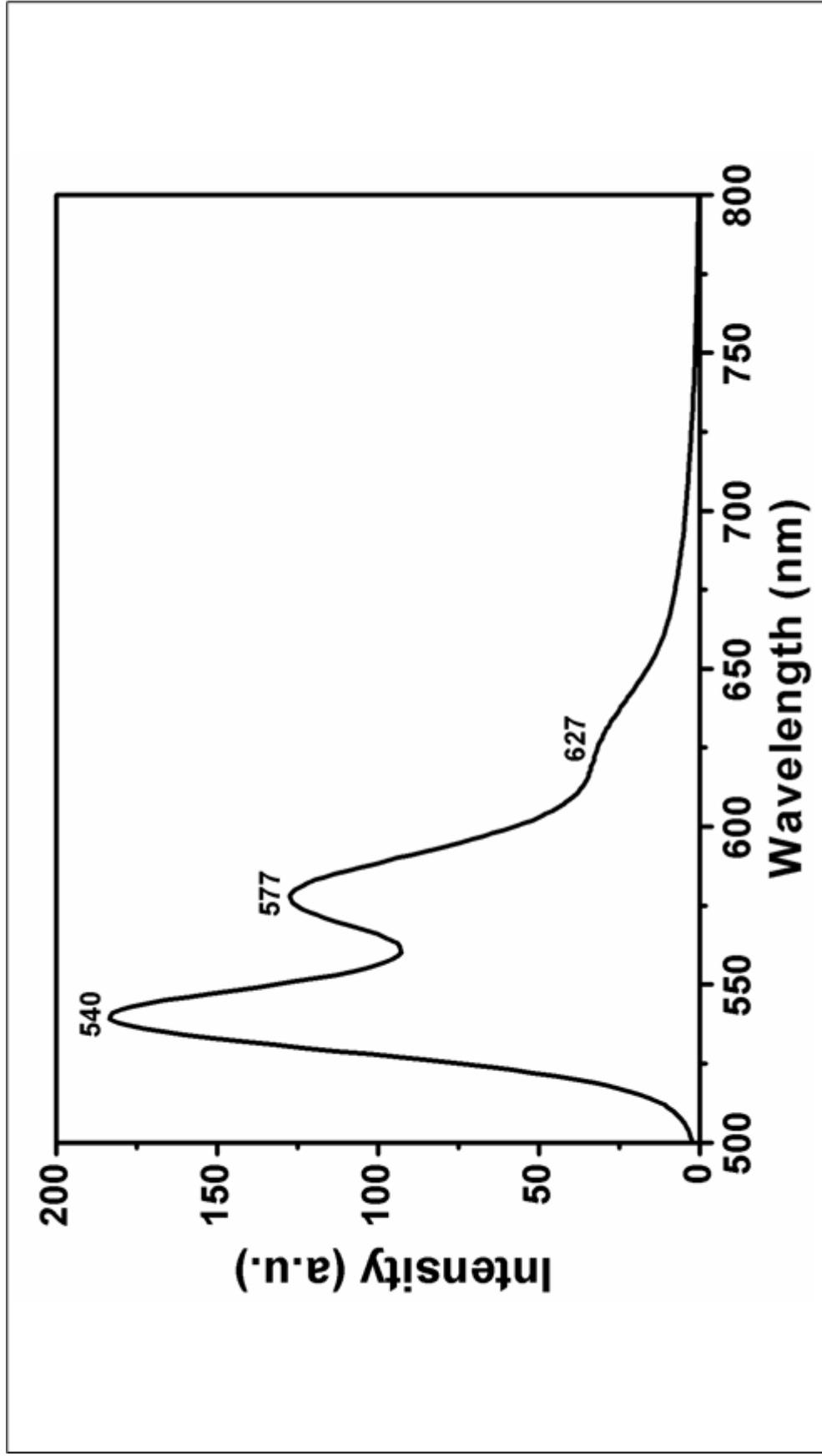




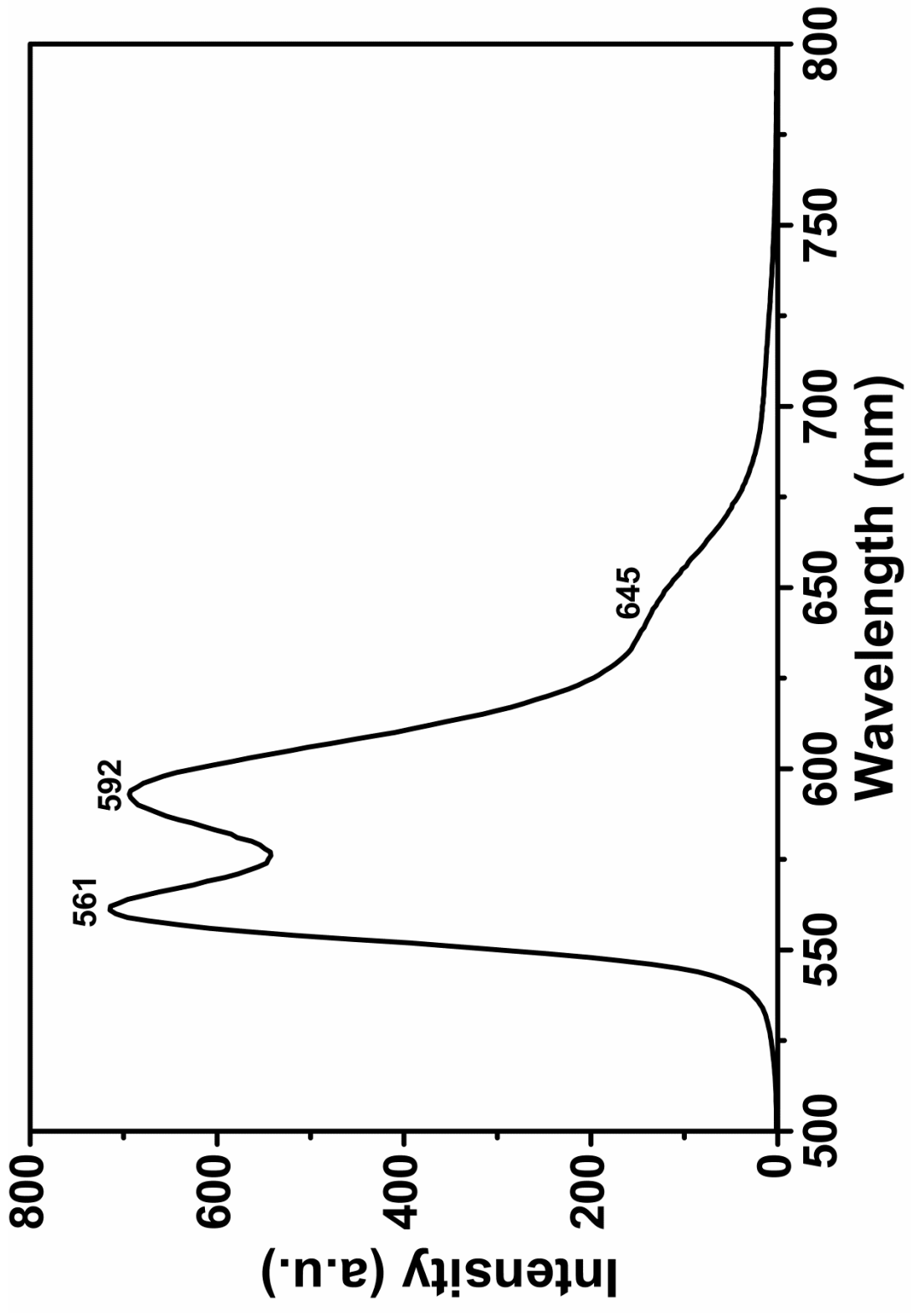


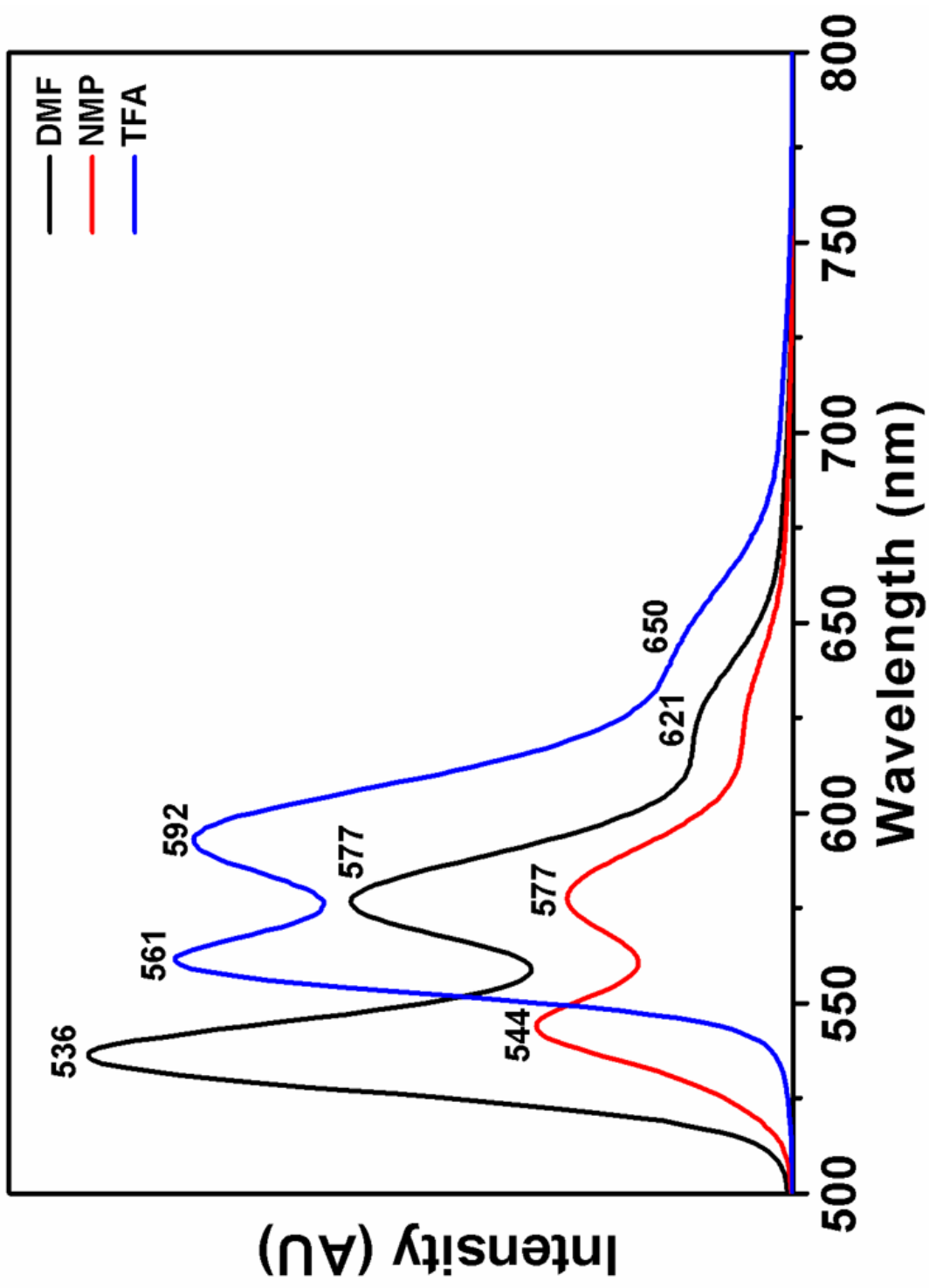


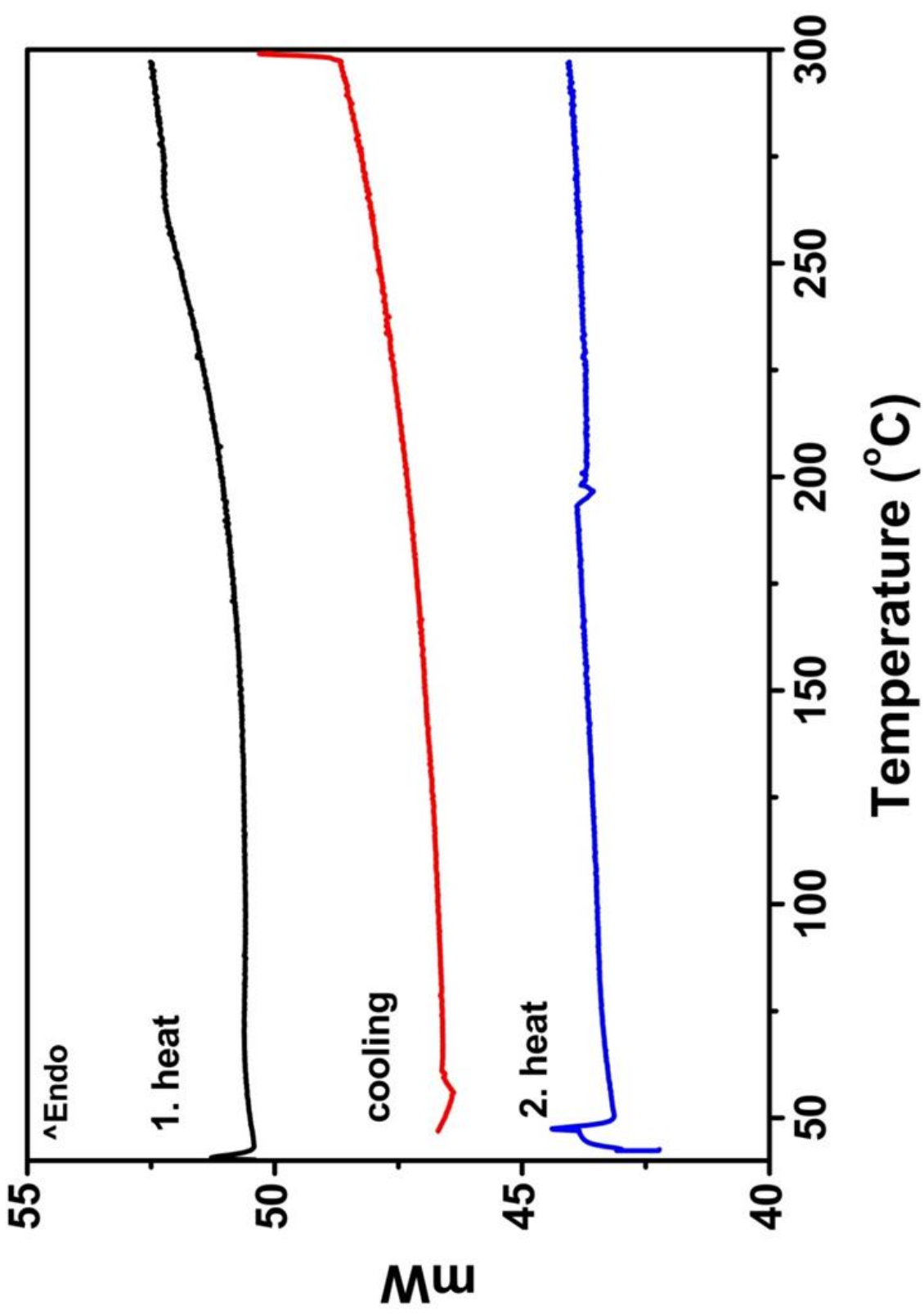


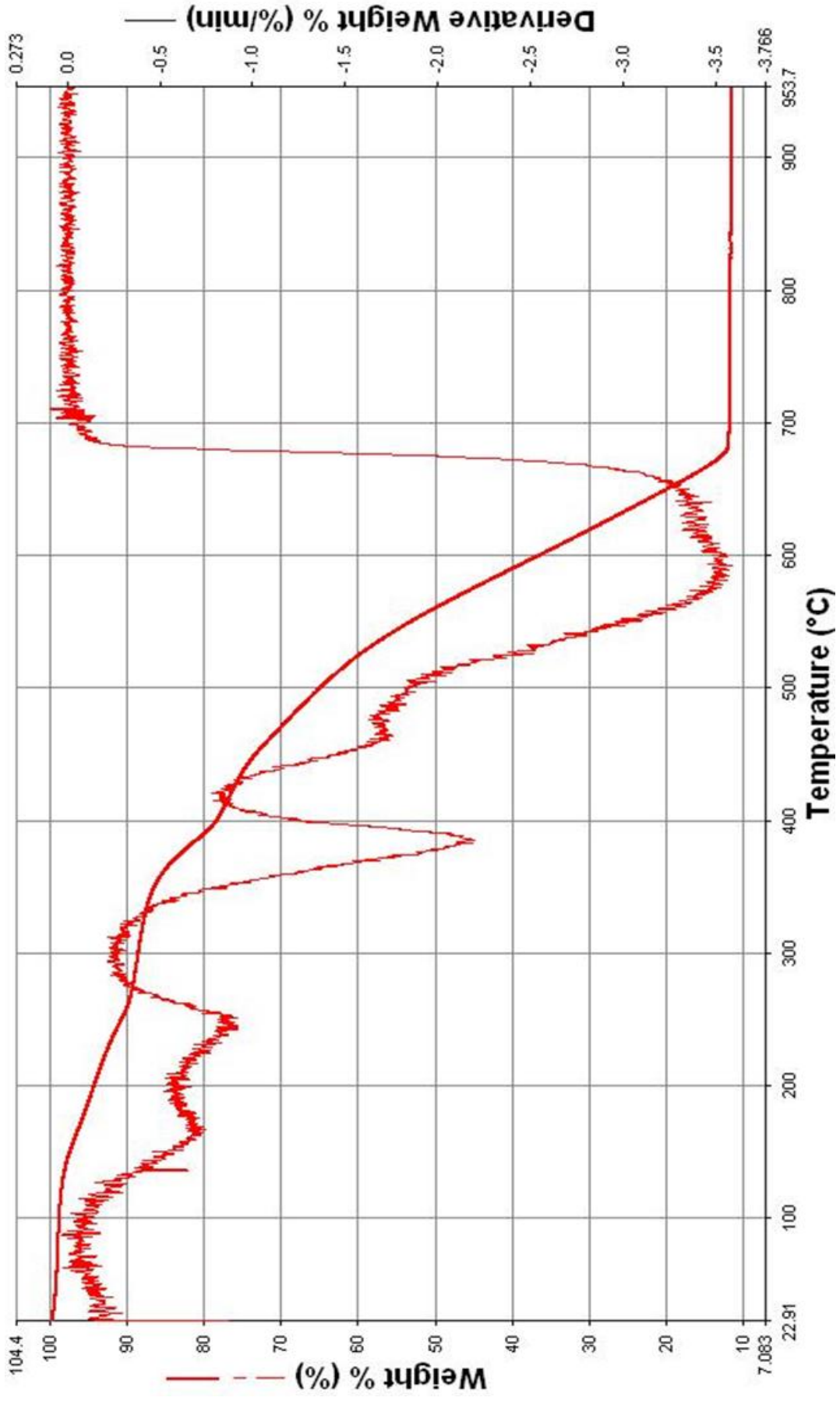












## Chapter 5

### RESULTS AND DISCUSSION

#### 5.1 Synthesis and Characterization

The perylene dye compound was synthesized in a one step process by a condensation reaction mechanism. Perylene-3,4,9,10-tetracarboxylic dianhydride was converted to perylene diimide via condensation with amine (4,6-diamino-2-pyrimidinethiol) and solvent mixture of *m*-cresol and isoquinoline as shown in Scheme 3.1.

The solubility properties of the synthesized perylene diimide are presented in Table 5.1 in various solvents.

Table 5.1 Solubility of the synthesized perylene derivative (T-PDI)

Solvents	Solubility/Color
DMF	(- +)* / Red
NMP	(- +)* / Pale red
DMSO	(- +)* / Pale red
TFA	(- +)* / Dark Pink
<i>m</i> -cresol	(- +)* / Red
CCl <sub>4</sub>	(- +)* / Pale red
DCM	(- -) / colourless
TCE	(- -) / colourless
Acetone	(- -) / colourless
Chloroform	(- -) / colourless

(- -): insoluble at room temperature; ((- +): slightly soluble at room temperature;  
\*: solubility increased upon heating at 60 °C.

The compound is partially soluble in DMF, NMP, DMSO, TFA, *m*-cresol and CCl<sub>4</sub> at room temperature and increased upon heating at 60 °C. It is insoluble in DCM, TCE, acetone and chloroform at room temperature. This is due to the symmetry and rigidity of the synthesized compound.

### 5.1.1 Analysis of IR Spectra

The FTIR spectrum of T-PDI completely represented the functional groups in the synthesized compound. Figure 4.3-4.5 shows the FTIR spectra of 4,6-Diamino-2-pyrimidinethiol, PDA and T-PDI, respectively.

The FTIR spectrum of 4,6-Diamino-2-pyrimidinethiol (Figure 4.3) shows the following characteristic bands at 3438 cm<sup>-1</sup>, 3393 cm<sup>-1</sup> (N-H stretch); 3062 cm<sup>-1</sup>, 3122 cm<sup>-1</sup>, 3250 cm<sup>-1</sup>(aromatic C-H stretch), 1630 cm<sup>-1</sup> (N-H bending), 1592 cm<sup>-1</sup> (aromatic C=C stretch), 798 cm<sup>-1</sup> (C-H bend).

The FTIR spectrum of PDA (Figure 4.4) shows the following bands: The FTIR Spectrum of PDA has shown characteristic bands at 3048 cm<sup>-1</sup>(aromatic C-H stretch), 1770 cm<sup>-1</sup> (anhydride C=O stretch), 1592 cm<sup>-1</sup> (aromatic C=C stretch), 1022 cm<sup>-1</sup> (C-O stretch), 805 cm<sup>-1</sup>, 731 cm<sup>-1</sup> (C-H bend).

The FTIR spectrum of T-PDI (Figure 4.5) shows characteristic bands at 3400 cm<sup>-1</sup> (N-H stretch); 3092 cm<sup>-1</sup> (aromatic C-H stretch); 1697 cm<sup>-1</sup> (imide C=O stretch); 1645 cm<sup>-1</sup> (N-H bending), 1585 cm<sup>-1</sup> (C=C stretch); 1330 cm<sup>-1</sup> (C-N stretch); 979 cm<sup>-1</sup> and 806 cm<sup>-1</sup> (C-H bend).

## 5.2. Absorption and Fluorescence Properties

The optical and electronic properties of perylene derivatives are unique and makes perylene dyes active in it's various application which include photovoltaic cells, laser dyes, chemical sensors etc. These properties are investigated by the absorption and emission spectra of the synthesized compound in polar protic solvent (TFA) and polar aprotic solvents (NMP, DMF) at  $1 \times 10^{-5}$  M concentration.

### 5.2.1 Analysis of UV-vis Absorption Spectra of T-PDI

Absorption spectrum of 4,6-Diamino-2-pyrimidin-thiol and PDA were studied in DMF (Figure 4.6 and 4.7). In Figure 4.6. two absorption bands observed at 352 nm and 369 nm. Absorption spectrum of PDA exhibits three characteristic bands at 452 nm, 482 nm and 516 nm in Figure 4.7.

The UV-vis absorption spectrum of T-PDI shows three characteristic bands. The absorption spectrum of T-PDI in DMF, before and after microfiltration is shown in Figure 4.7 and 4.8, respectively. In Figure 4.8., five absorption bands were observed at 463, 494, 511, 528 and 554 nm. After microfiltration, the weak peak at 554 nm disappears which indicates aggregation of lower concentration as shown in Figure 4.8. and three characteristic absorption praks at 462 nm, 492 nm and 528 nm obderved in DMF after microfiltration with 0.2 $\mu$ m (Figure 4.9).

Figure 4.10 and 4.11 shows three major characteristic absorption peaks of T-PDI at 460 nm, 490 nm, and 527 nm in NMP. The three characteristics  $0 \rightarrow 2$ ,  $0 \rightarrow 1$ , and  $0 \rightarrow 0$  peaks represent the pi-pi electronic transitions of aromatic perylene.

The absorption spectrum of T-PDI in TFA is shown in Figure 4.12. Similar with the result of T-PDI in NMP, the characteristic perylene diimide peaks at 465 nm, 495

nm, and 533 nm were observed. There are 6 nm bathochromic shift observed in TFA by comparing DMF and NMP.

### **5.2.2 Analysis of Emission Spectra of T-PDI**

The emission spectrum of T-PDI (Figure 4.14) shows three characteristic emission peaks at 536 nm, 576 nm and 626 nm in polar aprotic solvent, DMF. The spectrum shows the traditional emission peaks of 0→0, 0→1 and 0→2 transitions of perylene chromophore. After microfiltration as shown in Figure 4.15, slight changes occur in spectral shape and emission intensity decreases.

The emission spectra of T-PDI in NMP before and after microfiltration are reported in Figure 4.16 and 4.17, respectively. They show three major characteristic emission peaks at 540 nm, 577 nm, and 628 nm. The spectral shape and peaks remains the same after microfiltration.

The emission spectrum of T-PDI in polar protic solvent, TFA (Figure 4.18) shows three major characteristic emission peaks at 561 nm, 592 nm and 645 nm. The maximum emission intensity is at 561 nm.

Almost no change observed in the emission spectra of T-PDI in aprotic solvents. On the other hand, 21 nm bathochromic shifts observed in protic solvent which is attributed hydrogen-bonding (Figure 4.13 and 4.19) .

### **5.3 Thermal Stability**

From Figure 4.20 and 4.21, the thermal analysis of T-PDI was investigated by differential scanning calorimetry, DSC (10 K/min<sup>-1</sup>) and thermogravimetry, TGA (5 K/min<sup>-1</sup>) techniques. No glass transition temperature was observed in the DSC run. The TGA thermogram showed high starting decomposition temperatures ( $T_d$ ) for the



compounds. T-PDI was stable up to 300 °C. It exhibited a rapid weight loss of 12 % between 300 °C and 391 °C. When T-PDI was heated to 900 °C, 88 % of the initial weight was lost and 12 % char yield was left behind. Thus, T-PDI shows a good thermal stability.

## Chapter 6

### CONCLUSION

In this thesis, a new perylene diimide dye T-PDI containing powerful binding site for metal ions was synthesized successfully. The synthetic product T-PDI was characterized by FTIR, UV-vis, emission, TGA and DSC techniques.

The solubility of T-PDI was limited in polar aprotic and protic solvents (DMF, DMSO, TFA etc.) as shown in Table 5.1., while it is insoluble in nonpolar solvents (chloroform).

Spectroscopic properties of T-PDI was investigated by UV-vis absorption and fluorescence spectroscopy. In the absorption spectra minor changes were observed either in aprotic or protic solvents. Only aggregation formation was detected in DMF. On the other hand, 21 nm bathochromic shifts was observed in protic solvent which is attributed hydrogen-bonding due to the strong hydrogen bond donating TFA (Figure 4.13 and 4.19).

T-PDI was thermally stable and no glass transition temperature was observed in the DSC run.

The high thermal and photostabilities, including important photonic properties, make the new dye a potential candidate for various photo-sensing applications.

As future work, the metal binding will be investigated in detail. Upon metal binding, changes in both photophysical and photochemical properties of sensitizers such as wavelength shift and intensity change in absorption and emission spectra is expected and makes it suitable for many other applications. The high absorptions, high quantum yields, light-emitting optical and photophysical processes make them exciting choices for various device architectures.

## REFERENCES

- [1] Wurthner F., (2004). Perylene Bisimide Dyes as Versatile Building Blocks for Functional Supramolecular Architectures. *Chem commu* , 1564-1579.
- [2] Kardos M.B., (1913). Aceanthrenchinon- and 1.9 - anthracene derivatives. *Dtsch. Chem. Ges.*, 46, 2086-2091.
- [3] Liebermann C., & Kardos M. B., (1914). *Dtsch. chem. Ges.*, 47, 1203-1210.
- [4] Kelly R.F., Shin W.S., Rybtchinski B., Sinks L.E & Wasielewski M.R., ( 2007). *J Am.Chem.Soc* 129.3173-3181.
- [5] Chen, Z. J., Wang, L. M., Zou, G., Zhang, L., Zhang, G. J., Cai, X. F., & Teng, M. S. (2012). Colorimetric and ratiometric fluorescent chemosensor for fluoride ion based on perylene diimide derivatives. *Dyes and Pigments*, 94(3), 410-415.
- [6] Pasaogullari, N., Icil, H., & Demuth, M. (2006). Symmetrical and unsymmetrical perylene diimides: Their synthesis, photophysical and electrochemical properties. *Dyes and pigments*, 69(3), 118-127.
- [7] Refiker, H., & İcil, H., (2011). Amphiphilic and chiral unsymmetrical perylene dye for solid-state dye-sensitized solar cells. *Turkish Journal of Chemistry*, 35(6), 847-859.

- [8] Würthner, F., & Stolte, M. (2011). Naphthalene and perylene diimides for organic transistors. *Chemical Communications*, 47(18), 5109-5115.
- [9] Che, Y., Datar, A., Balakrishnan, K., & Zang, L. (2007). Ultralong nanobelts self-assembled from an asymmetric perylene tetracarboxylic diimide. *Journal of the American Chemical Society*, 129(23), 7234-7235.
- [10] Li, X., Sinks, L. E., Rybtchinski, B., & Wasielewski, M. R. (2004). Ultrafast aggregate-to-aggregate energy transfer within self-assembled light-harvesting columns of zinc phthalocyanine tetrakis (perylene diimide). *Journal of the American Chemical Society*, 126(35), 10810-10811.
- [11] Li, H., Wu, J., Yin, Z., & Zhang, H. (2014). Preparation and applications of mechanically exfoliated single-layer and multilayer MoS<sub>2</sub> and WSe<sub>2</sub> nanosheets. *Accounts of chemical research*, 47(4), 1067-1075.
- [12] Ozser, M. E., Uzun, D., Elci, I., Icil, H., & Demuth, M. (2003). Novel naphthalene diimides and a cyclophane thereof: synthesis, characterization, photophysical and electrochemical properties. *Photochemical & Photobiological Sciences*, 2(3), 218-223.
- [13] Ping Y., Arindam C., Michael W. H., & David M. A. (2005). Self-Organized Perylene Diimide Nanofibers. *J. Phys. Chem. B* 109, 724-730.

- [14] Tian, Z., Shaller, A. D., & Li, A. D. (2009). Twisted perylene dyes enable highly fluorescent and photostable nanoparticles. *Chemical Communications*, (2), 180-182.
- [15] Chen, Y., Kong, Y., Wang, Y., Ma, P., Bao, M., & Li, X. (2009). Supramolecular self-assembly study of a flexible perylenetetracarboxylic diimide dimer in Langmuir and Langmuir–Blodgett films. *Journal of colloid and interface science*, 330(2), 421-427.
- [16] Jancy, B., & Asha, S. K. (2007). Hydrogen-bonding-induced conformational change from J to H aggregate in novel highly fluorescent liquid-crystalline perylenebisimides. *Chemistry of Materials*, 20(1), 169-181.
- [17] Yang, X. G., Yuan, H., Zhao, Q. L., Yang, Q., & Chen, X. H. (2009). Self-assembly constructed by perylene bisimide derivatives bearing complementary hydrogen-bonding moieties. *Journal of Central South University of Technology*, 16, 206-211.
- [18] Würthner, F., Thalacker, C., & Sautter, A. (1999). Hierarchical organization of functional perylene chromophores to mesoscopic superstructures by hydrogen bonding and  $\pi$ – $\pi$  interactions. *Advanced Materials*, 11(9), 754-758.
- [19] Fujita, M., Yazaki, J., & Ogura, K. (1990). Preparation of a macrocyclic polynuclear complex, [(en) Pd (4, 4'-bpy)]<sub>4</sub> (NO<sub>3</sub>)<sub>8</sub> (en= ethylenediamine, bpy= bipyridine), which recognizes an organic molecule in aqueous media. *Journal of the American Chemical Society*, 112(14), 5645-5647.

- [20] Würthner, F., & Sautter, A. (2000). Highly fluorescent and electroactive molecular squares containing perylene bisimide ligands. *Chemical Communications*, (6), 445-446.
- [21] Würthner, F., & Sautter, A. (2003). Energy transfer in multichromophoric self-assembled molecular squares. *Organic & biomolecular chemistry*, 1(2), 240-243.
- [22] Ventura, B., Langhals, H., Böck, B., & Flamigni, L. (2012). Phosphorescent perylene imides. *Chemical Communications*, 48(35), 4226-4228.
- [23] Müller, C. D., Falcou, A., Reckefuss, N., Rojahn, M., Wiederhirn, V., Rudati, P & Meerholz, K. (2003). Multi-colour organic light-emitting displays by solution processing. *Nature*, 421(6925), 829-833.
- [24] Langhals, H., Demmig, S., & Huber, H. (1988). Rotational barriers in perylene fluorescent dyes. *Spectrochimica Acta Part A: Molecular Spectroscopy*, 44(11), 1189-1193.
- [25] Ford, P. C., Cariati, E., & Bourassa, J. (1999). Photoluminescence properties of multinuclear copper (I) compounds. *Chemical reviews*, 99(12), 3625-3648.
- [26] Paez, B. A., Salvan, G., Scholz, R., Kampen, T. U., & Zahn, D. R. (2003). Interaction of metals with perylene derivatives as a model system for contact formation in OFET structures. SPIE's 48th Annual Meeting. *International Society for Optics and Photonics*, 210-217.

- [27] Würthner, F., Thalacker, C., Diele, S., & Tschierske, C. (2001). Fluorescent J-type aggregates and thermotropic columnar mesophases of perylene bisimide dyes. *Chemistry—A European Journal*, 7(10), 2245-2253.
- [28] Rodriguez-Morgade, M. S., Torres, T., Atienza-Castellanos, C., & Guldi, D. M. (2006). Supramolecular bis (rutheniumphthalocyanine)-perylene diimide ensembles: Simple complexation as a powerful tool toward long-lived radical ion pair states. *Journal of the American Chemical Society*, 128(47), 15145-15154.
- [29] Gomez, U., Leonhardt, M., Port, H., & Wolf, H. C. (1997). Optical properties of amorphous ultrathin films of perylene derivatives. *Chemical physics letters*, 268(1), 1-6.
- [30] Puech, K., Fröb, H., & Leo, K. (1997). Excimer dynamics in ultrathin organic films. *Journal of luminescence*, 72, 524-525.
- [31] Nagao, Y., Naito, T., Abe, Y., & Misono, T. (1996). Synthesis and properties of long and branched alkyl chain substituted perylenetetracarboxylic monoanhydride monoimides. *Dyes and pigments*, 32(2), 71-83.
- [32] Kaiser, H., Lindner, J., & Langhals, H. (1991). Synthesis of Nonsymmetrically Substituted Perylene Fluorescent Dyes. *ChemInform*, 22(23).
- [33] Langhals H. *Heterocycles*. (1995), 40 (1) 1477-1500.



- [34] Ma, J., Yin, L., Zou, G., & Zhang, Q. (2015). Regioisomerically Pure 1, 7-Dibromo-Substituted Perylene Bisimide Dyes: Efficient Synthesis, Separation, and Characterization. *European Journal of Organic Chemistry*, 2015(15), 3296-3302.
- [35] Clikeman, T. T., Bukovsky, E. V., Wang, X. B., Chen, Y. S., Rumbles, G., Strauss, S. H., & Boltalina, O. V. (2015). Core Perylene Diimide Designs via Direct Bay-and ortho-(Poly) trifluoromethylation: Synthesis, Isolation, X-ray Structures, Optical and Electronic Properties. *European Journal of Organic Chemistry*, 2015(30), 6641-6654.
- [36] Scholes, G. D. (2003). Long-range resonance energy transfer in molecular systems. *Annual review of physical chemistry*, 54(1), 57-87.
- [37] Förster, T. (1948). Intermolecular energy hike and fluorescence. *Annals of physics*, 437(1-2), 55-75.
- [38] Förster, T. (1959). 10th Spiers Memorial Lecture. Transfer mechanisms of electronic excitation. *Discussions of the Faraday Society*, 27, 7-17.
- [39] Rehm, D., & Weller, A. (1970). Kinetics of fluorescence quenching by electron and H-atom transfer. *Israel Journal of Chemistry*, 8(2), 259-271.
- [40] Marcus, R. A. (1956). On the theory of oxidation-reduction reactions involving electron transfer. *The Journal of Chemical Physics*, 24(5), 966-978.

- [41] Marcus, R. (1959). On the theory of electrochemical and chemical electron transfer processes. *Canadian Journal of Chemistry*, 37(1), 155-163.
- [42] Kavarnos, G. J. (1993). Fundamentals of photoinduced electron transfer. *Vch Pub.* New York.
- [43] Fritts, C. E. (1883). On a new form of selenium cell, and some electrical discoveries made by its use. *American Journal of Science*, (156), 465-472.
- [44] Tan Y., Liu J., Li Q., & Zhao K., (2014). Charge Transfer Properties of Organic Semiconductor Molecules of Perylene Derivative. *Chinese J. Struct. Chem.* Vol. 33, 335-345.
- [45] Shockley, W., & Queisser, H. J. (1961). Detailed balance limit of efficiency of p-n junction solar cells. *Journal of applied physics*, 32(3), 510-519.
- [46] Bai, Y. F., Zhao, K. Q., Hu, P., Wang, B. Q., & Shimizu, Y. (2009). Synthesis of amide group containing triphenylene derivatives as discotic liquid crystals and organic gelators. *Molecular Crystals and Liquid Crystals*, 509(1), 60-802.
- [47] Osswald, P., & Würthner, F. (2007). Effects of bay substituents on the racemization barriers of perylene bisimides: resolution of atropo-enantiomers. *Journal of the American Chemical Society*, 129(46), 14319-14326.

## **APPENDIX**

## **Appendix A: Curriculum Vitae**

### **AKPAN, COURAGE IBORO**

No. 13. Sakarya road, Famagusta. North Cyprus via mersin 10, Turkey

+905338528503

[courageakpan11@gmail.com](mailto:courageakpan11@gmail.com)

---

#### **CAREER OBJECTIVE**

A highly committed, personable individual seeking a challenging and responsible position in an organization where good management, hard work, effective services and excellent opportunities exist both to broaden my experience and to contribute to the growth and development of the organization.

#### **PERSONAL DATA**

Date of Birth: 11<sup>th</sup> June 1986

Sex: Male

Marital status: Single

Nationality: Nigerian

State of Origin: Akwalbom state

L.G.A: OrukAnam

#### **ACADEMIC/EDUCATIONAL QUALIFICATIONS**

- Masters of Science in Chemistry (Hons) – July 2016  
**Eastern Mediterranean University, North Cyprus (2014-2016)**
- Bachelor of Science in Biochemistry (Hons)2<sup>nd</sup> Class Division  
**Ambrose Alli University, Ekpoma. Edo state (2004-2008)**
- National Examination Council, NECO  
**Blessing Sec. School, Ekpoma. Edo state (1998-2004)**
- Primary School Leaving Certificate  
**Brighter TomorrowN/P School.Irrua. Edo state (1992-1998)**

#### **PROFESSIONAL CERTIFICATE**

Nigeria Institute of Management (NIM) Chartered

- Graduate Member – 2010

#### **WORK EXPERIENCE**

- National Youth Service Corps (NYSC) 2009-2010  
National Red Cross Society – Coordinator

Government Sec. School, Kadarko.Kaura LGA. Kaduna. Nigeria

- Chemistry Tutor (2011-2013)  
The Zion Place College  
Lagos, Nigeria.

## **SKILLS**

Proficient in MS Office Application and Corel

Excellent communication and interpersonal skills with high level of enthusiasm and ability to work

## **PERSONAL VALUES**

- Integrity
- Hard work
- Creativity
- Team spirit

## **HOBBIES**

Reading and Research making

## **REFEREES**

- **PROFESSOR DR ICIL HURIYE**  
Chemistry Department  
Eastern Mediterranean University, North Cyprus  
Tel: +(90) 392-630-1085 Fax: +(90) 392-365-2545  
E-Mail: Huriye.icil@emu.edu.tr
- **PROFESSOR DR K. E. EKPO**  
Biochemistry Department  
Ambrose Alli University.Ekpoma. Edo state  
+2348056174860
- **MR OSAGIEDE STEPHEN**  
University Health Centre,  
University of Benin,  
Benin, Nigeria  
+2348143421071